

Update on Testing the Isotropy of the Properties of Gamma-Ray Bursts

Jakub Řípa,^{1,2,3} Arman Shafieloo,^{4,5*}

¹*Astronomical Institute of Charles University, V Holešovičkách 2, CZ-180 00 Prague 8, Czech Republic*

²*MTA-Eötvös University Lendület Hot Universe Research Group, Pázmány Péter sétány 1/A, Budapest, 1117, Hungary*

³*Institute of Physics, Eötvös University, Pázmány Péter sétány 1/A, Budapest, 1117, Hungary*

⁴*Korea Astronomy and Space Science Institute, Daejeon 305-348, Korea*

⁵*University of Science and Technology, Daejeon 34113, Korea*

Accepted XXX. Received YYY; in original form ZZZ

ABSTRACT

Previously we proposed a novel method to inspect the isotropy of the properties of gamma-ray bursts (GRBs) such as their duration, fluences and peak fluxes at various energy bands and different time scales, complementary to existing studies of spatial distribution of GRBs by other authors. The method was then applied on the *Fermi* GBM Burst Catalog containing 1591 GRBs and except one particular direction where we noticed some hints of violation from statistical isotropy, the rest of the data showed consistency with isotropy. In this work we apply our method with some minor modifications to the updated *Fermi*/GBM data sample containing 2266 GRBs, thus $\sim 40\%$ larger. We also test two other major GRB catalogs, the BATSE Current GRB Catalog of the *CGRO* satellite containing ~ 2000 bursts and the *Swift*/BAT Gamma-Ray Burst Catalog containing ~ 1200 bursts. The new results using the updated data are consistent with our previous findings and no statistically significant anisotropic feature in the observed properties of these samples of all GRBs is found.

Key words: gamma-ray burst: general – cosmology: large-scale structure of Universe – methods: data analysis – methods: statistical

1 INTRODUCTION

The sky distribution of Gamma-Ray Bursts (GRBs) (Piran 2004; Mészáros 2006; Vedrenne & Atteia 2009; Kouveliotou et al. 2012; Gomboc 2012; Kumar & Zhang 2015; Dai et al. 2017; Willingale & Mészáros 2017) has been tested intensively and the early works claimed that they were distributed isotropically (Meegan et al. 1992; Briggs et al. 1996; Tegmark et al. 1996). As more observational data increased and various methods were applied, it was claimed that the group of short GRBs ($T_{90} < 2$ s) (Balázsz et al. 2003), which originate in mergers of compact objects such as neutron stars (Paczynski 1986; Eichler et al. 1989; Berger 2014; Abbott et al. 2017a,b,c), was distributed anisotropically (Balázsz et al. 1998, 1999; Magliocchetti et al. 2003; Vavrek et al. 2008; Tarnopolski 2017), where the T_{90} is the duration during which 90% of the detected counts from a GRB is accumulated (Kouveliotou et al. 1993). However, several other works claimed different results (Mészáros et al. 2000a,b; Litvin et al. 2001; Bernui et al.

2008; Veres et al. 2010; Ukwatta & Woźniak 2016). The works which analyzed GRBs of duration $2\text{ s} \lesssim T_{90} \lesssim 10\text{ s}$ found that also these bursts were distributed anisotropically (Mészáros et al. 2000a,b; Litvin et al. 2001; Vavrek et al. 2008; Veres et al. 2010). However, see works by Mészáros & Štoček (2003); Ukwatta & Woźniak (2016) which came to different conclusion. Anisotropical distribution on the sky was also proclaimed for very short GRBs ($T_{90} \leq 100\text{ ms}$) (Cline et al. 2005; Ukwatta & Woźniak 2016). On the other hand, the group of long GRBs ($T_{90} > 2\text{ s}$), which are associated with the collapses of massive stars (Fruchter et al. 2006; Woosley & Bloom 2006), were found to be distributed isotropically (Balázsz et al. 1998, 1999; Mészáros et al. 2000a,b; Magliocchetti et al. 2003; Vavrek et al. 2008; Tarnopolski 2017; Ukwatta & Woźniak 2016), however see Mészáros & Štoček (2003), which came to a different conclusion. Papers Mészáros et al. (2009a,b); Mészáros (2017, 2018) summarize these efforts.

Horváth et al. (2014, 2015) studied the spatial distribution of GRBs with known redshift and they concluded that they found a statistically significant clustering at the redshift range of $1.6 < z \leq 2.1$ of the size of about 2000–

* E-mail: shafieloo@kasi.re.kr

3000 Mpc. However, the work [Ukwatta & Woźniak \(2016\)](#) also analyzed GRBs with measured redshift concluded that an evidence of a significant clustering was not found. Implications of the results obtained by [Horváth et al. \(2014\)](#) on the Cosmological Principle are discussed by [Li & Lin \(2015\)](#). [Balázs et al. \(2015, 2018\)](#) found an over-density of GRBs in the redshift range of $0.78 < z < 0.86$ (comoving distance of 2770 Mpc), which forms a ring-like shape displayed by 9 GRBs with a diameter of 1720 Mpc. Other recent works which study the spatial distribution of GRBs with known redshift were done by [Raikov et al. \(2010\)](#); [Shirokov et al. \(2017\)](#).

The isotropy or homogeneity of the Universe has been intensively analyzed also using various observations other than GRBs, for example: supernovae Ia ([Colin et al. 2011](#); [Feindt et al. 2013](#); [Appleby et al. 2015](#); [Javanmardi et al. 2015](#)), galaxies and clusters of galaxies ([Frith et al. 2005a,b](#); [Gott et al. 2005](#); [Hogg et al. 2005](#); [Kashlinsky et al. 2008](#); [Scrimgeour et al. 2012](#); [Fernández-Cobos et al. 2014](#); [Appleby & Shafieloo 2014](#); [Kroupa 2015](#); [Javanmardi & Kroupa 2017](#); [Sokolov et al. 2018](#)), active galactic nuclei ([Tiwari & Jain 2018](#)), HI line sources ([Rudnick et al. 2007](#); [Avila et al. 2018](#)), groups of quasars ([Clowes et al. 2013](#); [Nadathur 2013](#)), cosmic microwave background ([Hinshaw et al. 1996](#); [Planck Collaboration et al. 2014, 2016](#)).

In our previous work [Řípa & Shafieloo \(2017\)](#) we proposed a new method to test the isotropy of the observed properties of GRBs such as their duration, fluences and peak fluxes at various energy bands and different time scales. This approach is novel because all the previous studies based on the GRB data tested only the distribution of the number densities of GRBs, but not their observed properties. In this paper we apply almost the same method, but with slight improvement of its sensitivity, to the considerably updated *Fermi* / Gamma-ray Burst Monitor (GBM) data sample, which is larger by $\sim 40\%$. Herein we also test the Burst And Transient Source Experiment (BATSE) Current GRB Catalog of the *Compton Gamma Ray Observatory (CGRO)* satellite containing more than 2000 GRBs and the *Swift* / Burst Alert Telescope (BAT) Gamma-Ray Burst Catalog containing more than 1200 GRBs.

The paper is organized as follows. Section 2 describes the used data samples. Section 3 details the used methodology. The results are presented in Section 4 and discussed in Section 5. The last Section 6 summarizes our conclusions.

2 DATA SAMPLES

Three catalogs are examined in this work. The first one is the database of the GBM instrument ([Meegan et al. 2009](#)) of the *Fermi* satellite¹ ([Atwood & GLAST Collaboration 1994](#)). Particularly, we employ the FERMIGBRST - Fermi GBM Burst Catalog² ([Goldstein et al. 2012](#); [Paciesas et al. 2012](#); [Gruber et al. 2014](#); [von Kienlin et al. 2014](#); [Narayana Bhat et al. 2016](#)), which is being constantly

¹ <http://fermi.gsfc.nasa.gov/>

² <https://heasarc.gsfc.nasa.gov/W3Browse/fermi/fermigbrst.html>

updated and which is one of the most complete burst catalog to date.

The second one is the database of the BATSE instrument ([Fishman et al. 1985](#)) of the CGRO³ ([Gehrels et al. 1993](#)). Particularly, we employ the BATSE Current Gamma-Ray Burst Catalog⁴. For details see also the previous BATSE catalogs: 1B ([Fishman et al. 1994](#)), 3B ([Meegan et al. 1996](#)), 4B ([Meegan et al. 1998](#)), and 4Br ([Paciesas et al. 1999](#)).

The third one is the database of the BAT instrument ([Barthelmy et al. 2005](#)) of the *Neil Gehrels Swift Observatory*⁵ ([Swift](#)) ([Gehrels et al. 2004](#)). Particularly, we employ the *Swift*/BAT Gamma-Ray Burst Catalog⁶, which is being constantly updated.

2.1 *Fermi*/GBM sample

Compared to our previous work [Řípa & Shafieloo \(2017\)](#), which used *Fermi*/GBM sample containing 1591 GRBs, in this article we use updated sample which contains $\sim 40\%$ larger number of GRBs. In this updated sample there is 2271 GRBs with the first one detected on 2008/07/14 and the last one detected on 2018/02/25. The following observables from the catalog are applied in our study:

- Galactic longitude l ($^{\circ}$), in the catalog denoted as *LII*.
- Galactic latitude b ($^{\circ}$), in the catalog denoted as *BII*.
- GRB duration T_{90} (s) measured in the energy range of 50–300 keV.
- Photon peak fluxes F_{64} , F_{256} , and F_{1024} ($\text{ph cm}^{-2} \text{s}^{-1}$) on the 64-ms, 256-ms, and 1024-ms timescales in the energy range of 10–1000 keV and in the catalog denoted as *Flux_64*, *Flux_256*, and *Flux_1024*, respectively.
- Photon peak fluxes $F_{64,B}$, $F_{256,B}$, and $F_{1024,B}$ ($\text{ph cm}^{-2} \text{s}^{-1}$) on the 64-ms, 256-ms, and 1024-ms timescales in the energy range of 50–300 keV and in the catalog denoted as *Flux_BATSE_64*, *Flux_BATSE_256*, and *Flux_BATSE_1024*, respectively.
- Fluence S (erg cm^{-2}) is the time integrated flux over the whole duration of a burst in the energy range of 10–1000 keV and in the catalog denoted as *Fluence*.
- Fluence S_B (erg cm^{-2}) is the time integrated flux over the whole duration of a burst in the energy range of 50–300 keV and in the catalog denoted as *Fluence_BATSE*.

Five GRBs have the T_{90} duration measured in a different energy range than the nominal range 50–300 keV or they have fluence and peak fluxes measured in a different energy range than the nominal one 10–1000 keV, therefore we removed those five GRBs from our data sample. For all remaining 2266 GRBs the galactic coordinates, T_{90} duration, all peak fluxes and fluences are measured, hence all of them (regardless of their duration, spectral properties, luminosity or measured redshift) define the whole *Fermi*/GBM sample and are used in our analysis.

³ <https://heasarc.gsfc.nasa.gov/docs/cgro/cgro/>

⁴ <https://gammaray.nsstc.nasa.gov/batse/grb/catalog/current/index.html>

⁵ <https://swift.gsfc.nasa.gov>

⁶ <https://swift.gsfc.nasa.gov/results/batgrbcatalog/index.html>

2.2 CGRO/BATSE sample

The BATSE Current Gamma-Ray Burst Catalog contains 2702 GRBs with the first burst on 1991/04/21, the last one on 2000/05/26. The following observables from the catalog are applied in our study:

- Galactic longitude l ($^{\circ}$), in the catalog denoted as *LII*.
- Galactic latitude b ($^{\circ}$), in the catalog denoted as *BII*.
- GRB duration T_{90} (s).
- Photon peak fluxes $F_{64,B}$, $F_{256,B}$, and $F_{1024,B}$ ($\text{ph cm}^{-2} \text{s}^{-1}$) on the 64-ms, 256-ms, and 1024-ms timescales in the energy range of 50–300 keV and in the catalog denoted as *Flux_64*, *Flux_256*, and *Flux_1024*, respectively.
- Fluence S_1 (erg cm^{-2}) is the time integrated flux over the duration of the burst in the energy range of 20–50 keV and in the catalog denoted as *Fluence_1*.
- Fluence S_2 (erg cm^{-2}) is the time integrated flux over the duration of the burst in the energy range of 50–100 keV and in the catalog denoted as *Fluence_2*.
- Fluence S_3 (erg cm^{-2}) is the time integrated flux over the duration of the burst in the energy range of 100–300 keV and in the catalog denoted as *Fluence_3*.
- Fluence S_4 (erg cm^{-2}) is the time integrated flux over the duration of the burst at energy >300 keV and in the catalog denoted as *Fluence_4*.

For the sake of completeness, it should be mentioned that not all of the above-mentioned observables are independent (Bagoly et al. 1998, 2009; Borgonovo & Björnsson 2006). The duration T_{50} is not investigated in this work because it strongly correlates with commonly used T_{90} .

All 2702 GRBs in the catalog have measured galactic coordinates l and b . The number of GRBs in this catalog with a measured given observable is following: T_{90} (2037), $F_{64,B}$ (2132), $F_{256,B}$ (2132), $F_{1024,B}$ (2132), S_1 (2100), S_2 (2118), S_3 (2127), and S_4 (1752). If an observable is measured then it is included in our analysis, therefore these are the sizes of the whole CGRO/BATSE samples (no restriction is put on the bursts' duration, spectral properties, luminosity or measured redshift).

2.3 Swift/BAT sample

The data sample of the *Swift*/BAT Gamma-Ray Burst Catalog, which we use in this work, contains 1223 GRBs with the first burst on 2004/12/17, the last one on 2018/05/14. The following GRB observables from the catalog are applied in our analysis:

- RA from the BAT refined position (J2000, deg), in the catalog denoted as *RA_ground*.
- DEC from the BAT refined position (J2000, deg), in the catalog denoted as *DEC_ground*. We converted RA and DEC to the galactic longitude l ($^{\circ}$) and latitude b ($^{\circ}$).
- GRB duration T_{90} (s).
- 1-s peak energy fluxes F_1 , F_2 , F_3 , F_4 , F_5 , F_6 , and F_7 ($\text{erg cm}^{-2} \text{s}^{-1}$) in the energy ranges of 15–25 keV, 25–50 keV, 50–100 keV, 100–150 keV, 100–350 keV, 15–150 keV and, 15–350 keV, respectively.

- Fluences S_1 , S_2 , S_3 , S_4 , S_5 , S_6 , S_7 (erg cm^{-2}) which are the time integrated fluxes over the duration of the whole burst T_{100} in the energy ranges of 15–25 keV, 25–50 keV, 50–100 keV, 100–150 keV, 100–350 keV, 15–150 keV and, 15–350 keV, respectively.

Two spectral models, used for the calculation of the energy fluxes and fluences, are given in the catalog: a simple power-law model, and a cutoff power-law model. The best-fit model was selected based on the record in the catalog. If the information about the best-fit model was not available then we selected the one with higher null probability of the model as recorded in the catalog.

Eleven events from 1223 GRBs in the used data sample are not localized, therefore we removed them from the analysis. One event GRB140716A was triggered twice (trigger numbers 604793 and 604792). In order to avoid any mistake related to the overall duration T_{90} , fluxes and fluences, we removed both triggers from the data sample. Therefore the remaining number of GRBs with determined position in the sample is 1210.

From this number of 1210 GRBs the number of bursts with measured a given observable is following: T_{90} (1197); F_1 , F_2 and F_4 – F_7 (1143); F_3 (1142); S_1 – S_7 (1177) and these are the sizes of the whole *Swift*/BAT data samples (no other restrictions were applied).

3 METHOD

Almost the same method, as proposed by Řípa & Shafieloo (2017), is applied in this work. We refer the reader to that paper to see details of the methodology. Here the method is described only briefly.

Instead of examining the number density of GRBs on the sky, as most of the previous studies did, the key idea of this method is to analyze the sky distribution of the properties of GRBs. Therefore our method do not test the spatial distribution of GRBs. Since our method tests solely the isotropy of the observed properties of GRBs, no conclusion is drawn about their spatial distribution. For example, the over-densities of GRBs claimed by Horváth et al. (2014, 2015), i.e. the Hercules Corona Borealis Great Wall or the Giant GRB Ring claimed by Balázs et al. (2015, 2018) or the anisotropic distribution of very short GRBs claimed by Cline et al. (2005); Ukwatta & Woźniak (2016) cannot be confirmed or rejected using this method.

In this article the method was slightly improved in order to increase the sensitivity in the performed statistical tests. Contrary to the original method, where the distributions of a given measured GRB property from large number of randomly spread patches on the sky were compared with a distribution of the same GRB property for the whole sky, herein we compare the distributions from the patches with the distributions obtained from the complement area of that patches. This methodology is based on the principles of the crossing statistic applied in different aspects in cosmology (Shafieloo et al. 2011; Colin et al. 2011; Shafieloo 2012a,b; Akrami et al. 2014).

Four different test statistics are applied to measure the differences between the distributions for a random patch and its complement. In order to infer the significance of potential anisotropies the obtained distributions of the test statistics

derived from the measured data are compared with the distributions of the test statistics for randomly shuffled data. This comparison of the measured data with the randomly shuffled once means in essence comparison of the measured data to the isotropically distributed hypothetical sample and thus it is a principal step in this procedure. The null hypothesis is that observed properties of GRBs are distributed isotropically and we are testing against this null hypothesis.

Shortly the main steps of the used method are following (for details see Řípa & Shafieloo (2017)). A thousand of randomly distributed patches on the sky of a fixed radius r is generated and afterwards their positions are kept fixed. Let $G_q(x)$ be the empirical distribution function of a given tested observable x of GRBs (e.g. $x = T_{90}$, S , F , etc.) in a given patch (the number of GRBs in the patch is q and it varies patch to patch). Let $F_p(x)$ be the empirical distribution function of the same tested GRB observable x in the complement area on the sky of the same patch (the number of GRBs in that complement area is p and it naturally also varies patch to patch).

Next, for each patch compare $G_q(x)$ and $F_p(x)$ by calculating four test statistics $\xi = D$, V , AD , or χ^2 , where D is the statistic of the two-sample Kolmogorov–Smirnov (K–S) test (Kolmogorov 1933; Smirnov 1939; Press et al. 2007), V is the statistic of the two-sample Kuiper test (Kuiper 1960; Press et al. 2007), AD is the statistic of the two-sample Anderson–Darling (A–D) test (Anderson & Darling 1952; Darling 1957; Pettitt 1976), and χ^2 is the statistic of the two-sample Chi-square test (Press et al. 2007). In case of χ^2 the frequencies in the binned data (with 10 number of bins) of the two samples (containing logarithmic values $\log x$) are compared instead of the comparison of the empirical distribution functions. For 1000 patches one obtains a distribution of 1000 values of ξ^m (superscript m denotes that the quantity is related to the actual measured data sample).

In the next step the measured data sample is randomly shuffled $n = 1000$ times, i.e. the values x_i of each measurement are randomly shuffled, however the measured positions of GRBs $\{l_i, b_i\}$ are kept fixed. For each patch on the sky the test statistic ξ^s is calculated comparing the distribution $G_q^s(x)$ of the shuffled data for GRBs in the given patch and the distribution $F_p^s(x)$ for the patch’s complement area (superscript s denotes that the quantity is related to the randomly shuffled data). For each statistic ξ we derive the limiting values ξ_5^s , ξ_1^s , and ξ_0^s which delimit the highest 5 %, 1 %, and 0 % of all ξ^s values from all patches in all randomly shuffled data, respectively. The value ξ_0^s is the maximum of the ξ^s values.

Next, the distributions of a given statistic ξ for the measured data and for all data shufflings are compared. Let count the number of patches N_i^m in the measured data for which $\xi^m > \xi_i^s$. The mean number of patches \bar{N}_i^s in the randomly shuffled data for which $\xi^s > \xi_i^s$ is $\bar{N}_i^s = 50$ and 10 for $i = 5$ and 1, respectively. If N_i^m is found to be much higher than the average numbers \bar{N}_i^s then it could indicate anisotropy in the measured data. One can calculate the probability (significance) P_i^N of finding at least N_i^m number of patches with $\xi^s > \xi_i^s$ in the randomly shuffled data as well.

This analysis is performed for several patch radii $r = 20^\circ, 30^\circ, 40^\circ, 50^\circ, 60^\circ$, for all tested GRB observables in our data samples and for all four test statistics $\xi = AD$, D , V ,

and χ^2 . Various patch radii are chosen to make the technique sensitive to potential underlying structures of various sizes. The variations in the GRB properties in a patch is limited by the counting statistics and can be reduced by increasing the patch size.

The routines *KSTWO* and *KUIPERTWO* of the IDL⁷ Astronomy Users library⁸ (Landsman 1993) for calculation of the D and V statistics were used. For calculation of the A–D statistic, our own code, written based on the *adk_1.0-2* package⁹ (Scholz 2012) of the R software¹⁰ (R Core Team 2013), was used.

4 RESULTS

This section covers the results obtained for all examined data samples.

4.1 Results - *Fermi*/GBM

Tables 2–5 summarize the results of all tested fluxes, fluences and duration of GRBs in the *Fermi*/GBM sample using the Kolmogorov–Smirnov statistic D , Kuiper V , Anderson–Darling AD , and Chi-square χ^2 statistics, respectively.

For any of the test statistic, any radius nor any tested GRB observable, the probabilities P_i^N never decreased below 5 %. Also there is no case of a patch, of a given radius and for a given tested GRB observable and given test statistic ξ in the measured data which gives ξ^m higher than the highest ξ^s for patches of all random data shufflings.

The results applied on the *Fermi*/GBM sample are fully consistent with isotropy confirming our previous findings.

4.2 Results - CGRO/BATSE

Tables 6–9 summarize the results of all tested fluxes, fluences and duration of GRBs in the CGRO/BATSE sample using the Kolmogorov–Smirnov statistic D , Kuiper V , Anderson–Darling AD , and Chi-square χ^2 statistics, respectively.

There was only one case from all the applied statistical tests when the probability P_i^N decreased below 5 %. It was for the χ^2 statistic, fluences S_1 , patch radii $r = 20^\circ$ and $i = 1$. The patch centers for which χ^{2m} , for the measured data, is higher than χ^{2s}_1 obtained from the randomly shuffled data and the significance $P_1^N \leq 5\%$ are shown in Fig. 1.

The mean number of patches \bar{N}_1^s in the randomly shuffled data for which $\chi^{2s} > \chi^{2s}_1$ should be $\bar{N}_1^s = 10$ because we applied 1000 sky patches. The actual measured data gives $N_1^m = 28$. The corresponding chance probability of finding at least 28 patches on the sky with $\chi^{2s} > \chi^{2s}_1$ in the randomly shuffled data is $P_1^N = 4.1\%$.

There is no case of a patch, of a given radius and for a given tested GRB observable and given test statistic ξ in

⁷ <http://www.harrisgeospatial.com/ProductsandSolutions/GeospatialProducts/IDL.aspx>

⁸ <http://idlastro.gsfc.nasa.gov/>

⁹ <https://cran.r-project.org/src/contrib/Archive/adk/>

¹⁰ <https://www.r-project.org>

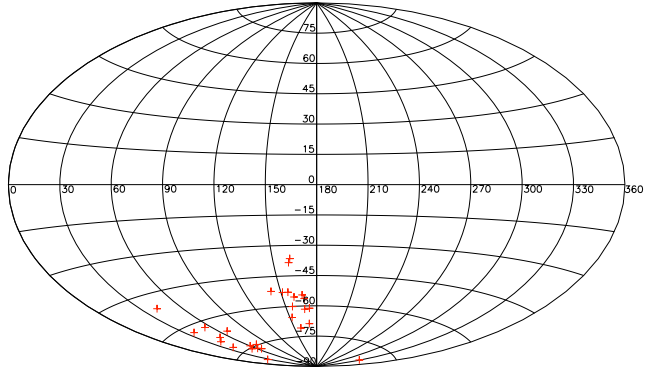


Figure 1. Plotted are the patch centers on the sky in Galactic Coordinates (Aitoff projection), for which the χ^2_m statistic, for the measured data, is higher than χ^2_s obtained from the randomly shuffled data and the significance P_i^N is below 5 %. The tested GRB property is fluences S_1 of the *CGRO/BATSE* data sample and the patch radii are $r = 20^\circ$. This is the only case in the *CGRO/BATSE* sample, for which the significance P_i^N is below 5 %.

the measured data which gives ξ^m higher than the highest ξ^s for patches of all random data shufflings.

In view of the fact that a large number of tests (eight different GRB observables, five different path radii and two different thresholds $i = 1, 5$) were applied, one occurrence of $P_i^N < 5\%$ does not imply any significant anisotropy. Therefore, the results applied on the *CGRO/BATSE* sample are fully consistent with isotropy, as well.

4.3 Results - *Swift/BAT*

Tables 10–13 summarize the results of all tested fluxes, fluences and duration of GRBs in the *CGRO/BATSE* sample using the Kolmogorov–Smirnov statistic D , Kuiper V , Anderson–Darling AD , and Chi-square χ^2 statistics, respectively. Quantities in the columns have the same meaning as in the previous Tables 2–9.

There were 18 cases with the chance probability $P_i^N \leq 5\%$, they are emphasized in boldface in the tables, and they were obtained for duration T_{90} (patch radii $r = 20^\circ$ – 60°), fluence S_1 ($r = 50^\circ$ and 60°) and peak flux F_2 ($r = 40^\circ$ and 50°). These are the cases for which the statistical properties of GRBs are mostly deviated from the randomness. Fig. 2 shows the patch centers on the sky for which a given test statistic ξ^m , for the measured data, is higher than ξ^s obtained from the randomly shuffled data and the significance $P_i^N \leq 5\%$.

The lowest chance probability obtained was for Chi-square statistic, duration T_{90} , patch radii $r = 40^\circ$, and threshold $i = 5$. The mean number of patches \bar{N}_5^s in the randomly shuffled data for which $\chi^{2s} > \chi_5^{2s}$ should be $\bar{N}_5^s = 50$ because we applied 1000 sky patches. The actual measured data gives $N_5^m = 136$. The corresponding chance probability of finding at least 136 patches on the sky with $\chi^{2s} > \chi_5^{2s}$ in the randomly shuffled data is $P_5^N = 1.7\%$.

There is no case of a patch, of a given radius and for a given tested GRB observable and given test statistic ξ in the measured data which gives ξ^m higher than the highest ξ^s for patches of all random data shufflings.

5 DISCUSSION

Table 1 demonstrates how the signal of a feature found in work Řípa & Shafieloo (2017) washed away with larger *Fermi*/GBM data sample used in this work and shows that the result do not point to any significant deviation from isotropy.

In case of the results obtained for the *Swift/BAT* a deeper discussion is needed. Eighteen tests gave the chance probability $P_i^N \leq 5\%$. Since we performed 600 statistical tests (15 tested GRB observables, 5 patch radii, 4 test statistics, and 2 limiting thresholds) it must be considered that the number of trials is high. However, not all of the tests are independent.

If we assume that there are $n = 600$ independent tests (trials), with the probability of success in a single test p , one can calculate the probability (*p-value*) of finding at least m successes in all trials from the binomial test. For details see for example Eq. (1) and (2) of Vavrek et al. (2008). From Tables 10 – 13 one can see that we obtained $m = 18$ for $p \leq 5\%$, $m = 9$ for $p \leq 3\%$, and $m = 4$ for $p \leq 2\%$. If we assume that $p = 5\%$ then we obtain for $m = 18$, $m = 9$, and $m = 4$ the following probabilities: *p-value* = 99.4 %, *p-value* = 99.4 %, and *p-value* = 99.8 %, respectively.

This is a coarse estimation because the tests are not independent. The number of independent tests (trials) is likely tens.

We obtained that in one test the lowest chance probability obtained was $P_5^N = 1.7\%$ (Chi-square statistic, duration T_{90} , and patch radii $r = 40^\circ$). However, for example, if the number of independent tests is 10 then for $p = 1.7\%$ the *p-value* of the binomial test is 16 %. If the number of independent tests is 20 then the *p-value* = 29 %. This suggests that a chance probability in a single test of 1.7 % is actually much more likely to occur by chance in one of the many tests used.

In order to estimate more precisely the chance probability of obtaining certain number of cases with P_i^N less or equal a given limit, we performed 20 Monte Carlo (MC) simulations. In each simulation we randomly shuffled the values of each observable in the measured database and then run the whole analysis with this shuffled database instead of the actual measured database. We obtained that in 17 out of 20 MC simulations there were $m \geq 18$ number of tests giving $P_i^N \leq 5\%$. Therefore one can say that there is approximately 85 % of chance probability of obtaining at least 18 times the probability $P_i^N \leq 5\%$ among the performed 600 tests in the isotropic randomized sample. We obtained the same percentage when we looked at the $m \geq 9$ number of tests giving $P_i^N \leq 3\%$ and when we looked at the $m \geq 4$ number of tests giving $P_i^N \leq 2\%$. This is a key argument suggesting that also the results obtained for the *Swift/BAT* data sample are consistent with isotropy.

Fig. 2 shows the patch centres for which a given statistic ξ^m , for the measured *Swift/BAT* data, is higher than ξ^s obtained from the randomly shuffled data and the significance $P_i^N \leq 5\%$, where $i=5$ or 1 . From that figure it can appear that because of the clustering of these patch centers these deviations might be real or due to systematic differences in how the distributions have been sampled. However, nearby patches do not contain independent samples because they have rather large radii and they overlap. If there are

Table 1. Comparison of some most significant results of several tests performed on the old (1591 GRBs in Řípa & Shafieloo (2017)) and the new (2266 GRBs in this work) data samples of *Fermi*/GBM for Kolmogorov–Smirnov statistic D and patch radii $r = 20^\circ$ demonstrating how the signal of a feature found in work Řípa & Shafieloo (2017) washed away with larger data sample.

| | old sample | | | | new sample | | | |
|----------|------------|---------|---------|---------|------------|---------|---------|---------|
| | N_5^m | P_5^N | N_1^m | P_1^N | N_5^m | P_5^N | N_1^m | P_1^N |
| F_{64} | 87 | 3.4 | 30 | 1.5 | 55 | 36.8 | 10 | 44.6 |
| S | 72 | 13.1 | 30 | 2.2 | 57 | 32.2 | 17 | 17.1 |
| S_B | 74 | 11.5 | 31 | 1.4 | 52 | 43.7 | 17 | 17.9 |

randomly few GRBs with, for example, very high or low flux close to each other then a bundle of nearby patches will contain these GRBs and the distributions of fluxes in all these patches will be affected. It is important to mention that similar “clustering” is seen also for the results of the MC simulations mentioned in the previous paragraph, where the whole analysis was run with randomly shuffled GRB properties in the catalog.

While discussing the results it should be mentioned that some selection effects could effect the results, for example the background variation on the sky or adjustment of the on-board trigger setting throughout the mission. On the other hand, since we found results consistent with isotropy possible selection effects would need to cancel out potential anisotropic features in the GRB properties.

6 CONCLUSIONS

We inspected the isotropy of the observed properties of GRBs (not the distribution of their number density on the sky) such as their duration, fluences and peak fluxes at various energy bands and different time scales by a novel method - in its original form proposed in our previous work - applied on three major GRB catalogs. The whole GRB samples containing bursts regardless of their duration, spectral properties, luminosity or measured redshift, were used. The conclusions are following:

- (i) We slightly improved the sensitivity of the original method proposed in work Řípa & Shafieloo (2017). Contrary to the original method, where the distributions of a given measured GRB property from large number of randomly spread patches on the sky were compared with a distribution of the same GRB property for the whole sky, herein we compare the distributions from the patches with the distributions obtained from the complement area of that patches.
- (ii) The method was applied to a considerably updated whole *Fermi*/GBM data sample containing 2266 GRBs, thus $\sim 40\%$ larger than the sample investigated in work Řípa & Shafieloo (2017). The signal of a feature found in work Řípa & Shafieloo (2017) washed away with larger data sample and the results are consistent with isotropy confirming our previous conclusions.

- (iii) The method was also applied to another large GRB dataset, the BATSE Current GRB Catalog of the *CGRO* satellite, which contains ~ 2000 bursts. The results based on the whole samples are consistent with isotropy as well.
- (iv) The last investigated whole GRB data sample is the *Swift*/BAT Gamma-Ray Burst Catalog containing ~ 1200 bursts. The localization accuracy of the *Swift*/BAT instrument is significantly better, ~ 2 arcmin compared to few degrees of *Fermi*/GBM or *CGRO*/BATSE. Therefore investigation of this sample is beneficial, too. The results are also consistent with isotropy.

ACKNOWLEDGEMENTS

We acknowledge use of the *Fermi*/GBM, *CGRO*/BATSE, and *Swift*/BAT data. This research has made use of data, software and/or web tools obtained from the High Energy Astrophysics Science Archive Research Center (HEASARC), a service of the Astrophysics Science Division at NASA/GSFC and of the Smithsonian Astrophysical Observatory’s High Energy Astrophysics Division. This work made use of procedures *KSTWO* and *KUIPERTWO* of the IDL software and its Astronomy Users library, and the package *adk_1.0-2* of the R software. We kindly thank to A. Mészáros and M. Tarnopolski for useful comments and suggestions. J.R. is supported by the Lendület LP2016-11 grant awarded by the Hungarian Academy of Sciences. The research has been supported by the European Union, co-financed by the European Social Fund (Research and development activities at the Eötvös Loránd University’s Campus in Szombathely, EFOP-3.6.1-16-2016-00023). A.S. would like to acknowledge the support of the National Research Foundation of Korea (NRF-2016R1C1B2016478). A.S. would like to acknowledge the support of the Korea Institute for Advanced Study (KIAS) grant funded by the Korea government.

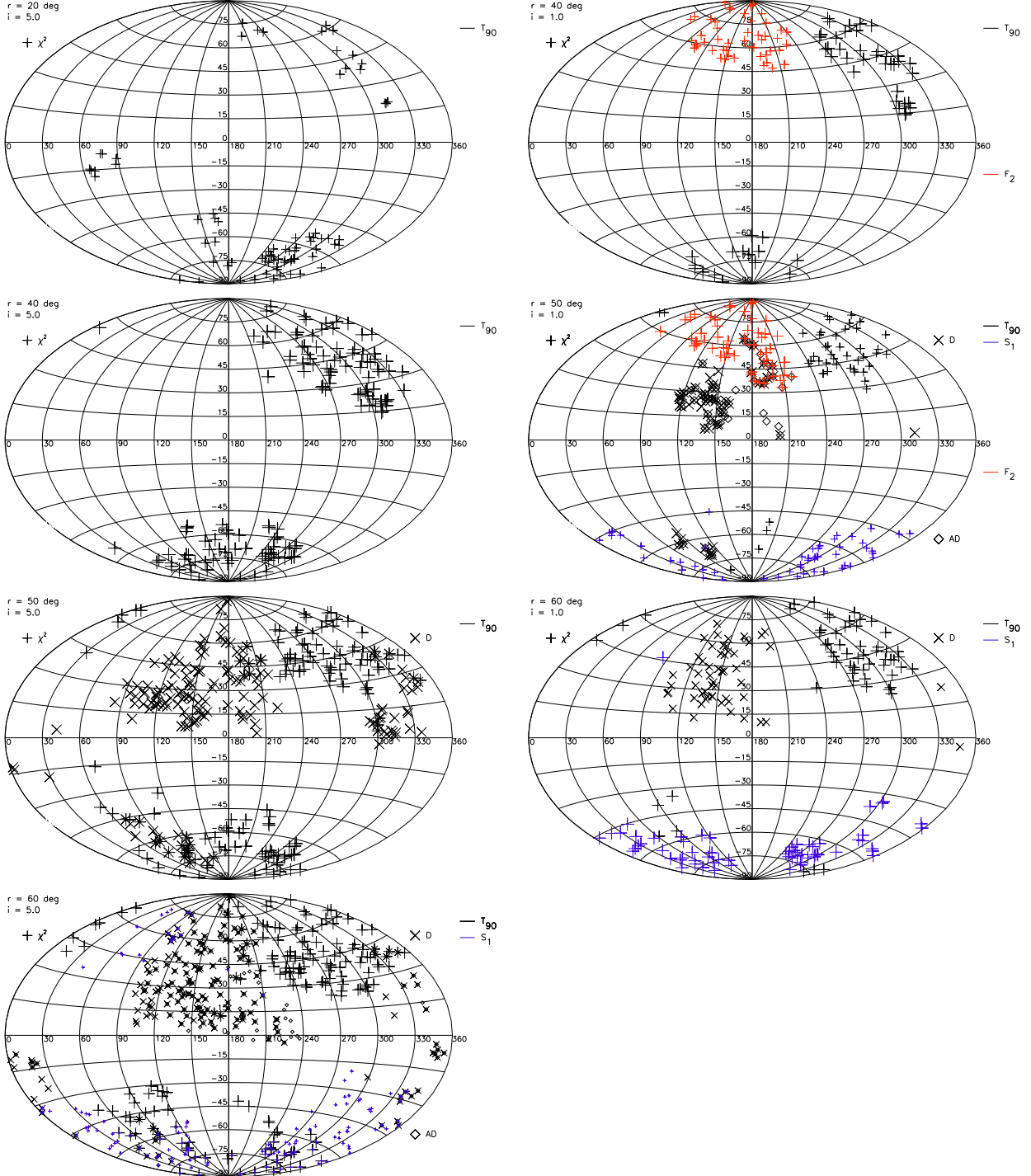


Figure 2. Plotted are the patch centers on the sky in Galactic Coordinates (Aitoff projection), for which the statistical properties of GRBs are mostly deviated from the randomness in the *Swift*/BAT data sample. The combined results for different statistics $\xi = D, AD$, or χ^2 : Kolmogorov–Smirnov’s D (crosses), Anderson–Darling’s AD (diamonds), or Chi-square χ^2 (pluses) are marked. The markers denote the centers of the patches for which a given statistic ξ^m , for the measured data, is higher than ξ_i^s obtained from the randomly shuffled data and the significance $P_i^N \leq 5\%$, where $i=5$ or 1 . The size of the markers is inverse proportional to the probability P_i^N . Different colors mean different properties of GRBs being tested. In different panels the results are plotted separately for different patch radii r and for different i .

Table 2. Results using the Kolmogorov–Smirnov statistic D for the *Fermi*/GBM sample.

| Obs. | r^* | $D_5^{s\dagger}$ | $N_5^{m\dagger}$ | $P_5^{N\#}$ | $D_1^{s\dagger}$ | $N_1^{m\dagger}$ | $P_1^{N\#}$ | $D_0^{s\dagger}$ | $D_0^{m\$}$ |
|--------------|-------|------------------|------------------|-------------|------------------|------------------|-------------|------------------|-------------|
| | (°) | | | (%) | | | (%) | | |
| T_{90} | 20 | 0.17 | 70 | 15.8 | 0.20 | 13 | 29.4 | 0.36 | 0.27 |
| T_{90} | 30 | 0.11 | 66 | 25.9 | 0.14 | 10 | 37.7 | 0.22 | 0.18 |
| T_{90} | 40 | 0.09 | 78 | 20.5 | 0.11 | 22 | 15.0 | 0.18 | 0.12 |
| T_{90} | 50 | 0.07 | 95 | 14.4 | 0.09 | 11 | 26.9 | 0.14 | 0.10 |
| T_{90} | 60 | 0.07 | 93 | 16.8 | 0.08 | 4 | 42.4 | 0.12 | 0.08 |
| S | 20 | 0.17 | 57 | 32.2 | 0.20 | 17 | 17.1 | 0.33 | 0.25 |
| S | 30 | 0.11 | 56 | 35.0 | 0.14 | 17 | 21.0 | 0.23 | 0.15 |
| S | 40 | 0.09 | 34 | 59.6 | 0.11 | 2 | 67.9 | 0.18 | 0.11 |
| S | 50 | 0.07 | 38 | 49.9 | 0.09 | 2 | 61.1 | 0.14 | 0.09 |
| S | 60 | 0.07 | 46 | 38.7 | 0.08 | 1 | 64.5 | 0.13 | 0.08 |
| S_B | 20 | 0.17 | 52 | 43.7 | 0.20 | 17 | 17.9 | 0.33 | 0.24 |
| S_B | 30 | 0.11 | 47 | 47.9 | 0.14 | 15 | 23.8 | 0.22 | 0.16 |
| S_B | 40 | 0.09 | 43 | 49.7 | 0.11 | 2 | 70.6 | 0.18 | 0.11 |
| S_B | 50 | 0.07 | 50 | 37.0 | 0.09 | 8 | 33.8 | 0.16 | 0.10 |
| S_B | 60 | 0.07 | 57 | 32.3 | 0.08 | 7 | 32.0 | 0.12 | 0.08 |
| F_{64} | 20 | 0.17 | 55 | 36.8 | 0.20 | 10 | 44.6 | 0.34 | 0.24 |
| F_{64} | 30 | 0.11 | 63 | 28.1 | 0.14 | 17 | 20.4 | 0.23 | 0.16 |
| F_{64} | 40 | 0.09 | 58 | 31.8 | 0.11 | 6 | 48.8 | 0.16 | 0.11 |
| F_{64} | 50 | 0.07 | 37 | 50.1 | 0.09 | 3 | 52.6 | 0.14 | 0.09 |
| F_{64} | 60 | 0.07 | 47 | 37.8 | 0.08 | 2 | 50.6 | 0.13 | 0.08 |
| F_{256} | 20 | 0.17 | 43 | 61.6 | 0.20 | 11 | 38.4 | 0.34 | 0.25 |
| F_{256} | 30 | 0.11 | 57 | 34.7 | 0.14 | 20 | 14.3 | 0.23 | 0.18 |
| F_{256} | 40 | 0.09 | 85 | 15.3 | 0.11 | 30 | 7.7 | 0.17 | 0.13 |
| F_{256} | 50 | 0.07 | 94 | 16.8 | 0.09 | 16 | 20.4 | 0.14 | 0.10 |
| F_{256} | 60 | 0.07 | 91 | 16.7 | 0.08 | 1 | 63.3 | 0.12 | 0.08 |
| F_{1024} | 20 | 0.17 | 32 | 83.3 | 0.20 | 9 | 48.6 | 0.35 | 0.24 |
| F_{1024} | 30 | 0.11 | 36 | 64.4 | 0.14 | 11 | 34.1 | 0.24 | 0.17 |
| F_{1024} | 40 | 0.09 | 29 | 66.6 | 0.11 | 1 | 81.4 | 0.17 | 0.11 |
| F_{1024} | 50 | 0.07 | 27 | 58.7 | 0.09 | 0 | 100.0 | 0.15 | 0.09 |
| F_{1024} | 60 | 0.07 | 25 | 59.8 | 0.08 | 0 | 100.0 | 0.12 | 0.08 |
| $F_{64,B}$ | 20 | 0.17 | 48 | 50.6 | 0.20 | 9 | 49.0 | 0.40 | 0.22 |
| $F_{64,B}$ | 30 | 0.11 | 40 | 59.0 | 0.14 | 5 | 61.2 | 0.26 | 0.16 |
| $F_{64,B}$ | 40 | 0.09 | 42 | 49.3 | 0.11 | 9 | 35.1 | 0.17 | 0.12 |
| $F_{64,B}$ | 50 | 0.07 | 40 | 47.4 | 0.09 | 3 | 53.1 | 0.14 | 0.09 |
| $F_{64,B}$ | 60 | 0.07 | 19 | 65.2 | 0.08 | 4 | 38.7 | 0.13 | 0.09 |
| $F_{256,B}$ | 20 | 0.17 | 33 | 81.1 | 0.20 | 5 | 72.4 | 0.36 | 0.21 |
| $F_{256,B}$ | 30 | 0.11 | 23 | 82.2 | 0.14 | 3 | 69.5 | 0.24 | 0.15 |
| $F_{256,B}$ | 40 | 0.09 | 19 | 79.7 | 0.11 | 1 | 77.1 | 0.17 | 0.11 |
| $F_{256,B}$ | 50 | 0.07 | 16 | 79.4 | 0.09 | 2 | 63.0 | 0.16 | 0.09 |
| $F_{256,B}$ | 60 | 0.07 | 13 | 73.4 | 0.08 | 4 | 42.4 | 0.12 | 0.08 |
| $F_{1024,B}$ | 20 | 0.17 | 29 | 86.6 | 0.20 | 2 | 91.7 | 0.33 | 0.20 |
| $F_{1024,B}$ | 30 | 0.11 | 26 | 78.3 | 0.14 | 0 | 100.0 | 0.24 | 0.13 |
| $F_{1024,B}$ | 40 | 0.09 | 8 | 95.0 | 0.11 | 0 | 100.0 | 0.18 | 0.09 |
| $F_{1024,B}$ | 50 | 0.07 | 27 | 61.5 | 0.09 | 0 | 100.0 | 0.14 | 0.09 |
| $F_{1024,B}$ | 60 | 0.07 | 17 | 68.0 | 0.08 | 1 | 65.1 | 0.13 | 0.08 |

* r are the radii of the patches.† D_5^s , D_1^s , and D_0^s delimit the highest 5%, 1%, and the maximum of all D^s values from all patches in all shuffled data.‡ N_i^m is the number of patches in the measured data for which $D^m > D_i^s$, where $i=5$ or 1.# P_i^N is the probability of finding at least N_i^m number of patches with $D^s > D_i^s$ in the randomly shuffled data, where $i=5$ or 1.§ D_0^m is the maximum value of the statistic in the measured data.**Table 3.** Results using the Kuiper statistic V for the *Fermi*/GBM sample.

| Obs. | r^* | $V_5^{s\dagger}$ | $N_5^{m\dagger}$ | $P_5^{N\#}$ | $V_1^{s\dagger}$ | $N_1^{m\dagger}$ | $P_1^{N\#}$ | $V_0^{s\dagger}$ | $V_0^{m\$}$ |
|--------------|-------|------------------|------------------|-------------|------------------|------------------|-------------|------------------|-------------|
| | (°) | | | (%) | | | (%) | | |
| T_{90} | 20 | 0.21 | 70 | 14.4 | 0.25 | 19 | 11.8 | 0.38 | 0.31 |
| T_{90} | 30 | 0.15 | 88 | 9.2 | 0.17 | 21 | 13.1 | 0.26 | 0.20 |
| T_{90} | 40 | 0.11 | 98 | 11.2 | 0.13 | 15 | 24.7 | 0.20 | 0.14 |
| T_{90} | 50 | 0.09 | 114 | 8.8 | 0.11 | 16 | 20.5 | 0.16 | 0.12 |
| T_{90} | 60 | 0.08 | 86 | 18.3 | 0.10 | 6 | 38.0 | 0.14 | 0.10 |
| S | 20 | 0.21 | 42 | 65.9 | 0.25 | 9 | 50.3 | 0.38 | 0.28 |
| S | 30 | 0.15 | 33 | 72.2 | 0.17 | 6 | 57.8 | 0.26 | 0.18 |
| S | 40 | 0.11 | 6 | 97.6 | 0.13 | 0 | 100.0 | 0.20 | 0.12 |
| S | 50 | 0.09 | 4 | 96.2 | 0.11 | 0 | 100.0 | 0.16 | 0.10 |
| S | 60 | 0.08 | 5 | 91.6 | 0.10 | 0 | 100.0 | 0.15 | 0.09 |
| S_B | 20 | 0.21 | 47 | 55.4 | 0.25 | 6 | 69.4 | 0.37 | 0.28 |
| S_B | 30 | 0.15 | 34 | 70.3 | 0.17 | 5 | 63.6 | 0.25 | 0.19 |
| S_B | 40 | 0.11 | 12 | 90.4 | 0.13 | 0 | 100.0 | 0.21 | 0.12 |
| S_B | 50 | 0.09 | 13 | 82.8 | 0.11 | 1 | 72.7 | 0.17 | 0.11 |
| S_B | 60 | 0.08 | 17 | 69.8 | 0.10 | 0 | 100.0 | 0.14 | 0.09 |
| F_{64} | 20 | 0.21 | 57 | 33.5 | 0.25 | 10 | 44.7 | 0.39 | 0.28 |
| F_{64} | 30 | 0.15 | 67 | 24.0 | 0.17 | 14 | 25.8 | 0.26 | 0.20 |
| F_{64} | 40 | 0.11 | 66 | 26.9 | 0.13 | 19 | 16.6 | 0.19 | 0.14 |
| F_{64} | 50 | 0.09 | 32 | 56.3 | 0.11 | 1 | 70.8 | 0.16 | 0.11 |
| F_{64} | 60 | 0.08 | 53 | 34.0 | 0.10 | 3 | 51.4 | 0.14 | 0.10 |
| F_{256} | 20 | 0.21 | 42 | 66.7 | 0.25 | 6 | 70.5 | 0.39 | 0.27 |
| F_{256} | 30 | 0.15 | 56 | 35.7 | 0.17 | 15 | 24.1 | 0.26 | 0.19 |
| F_{256} | 40 | 0.11 | 65 | 26.2 | 0.13 | 12 | 30.8 | 0.19 | 0.14 |
| F_{256} | 50 | 0.09 | 50 | 39.6 | 0.11 | 1 | 75.9 | 0.16 | 0.11 |
| F_{256} | 60 | 0.08 | 40 | 44.3 | 0.10 | 0 | 100.0 | 0.14 | 0.09 |
| F_{1024} | 20 | 0.21 | 35 | 79.5 | 0.25 | 9 | 50.0 | 0.36 | 0.29 |
| F_{1024} | 30 | 0.15 | 26 | 82.8 | 0.17 | 7 | 54.0 | 0.25 | 0.19 |
| F_{1024} | 40 | 0.11 | 10 | 93.8 | 0.13 | 3 | 65.7 | 0.21 | 0.14 |
| F_{1024} | 50 | 0.10 | 4 | 94.7 | 0.11 | 0 | 100.0 | 0.16 | 0.10 |
| F_{1024} | 60 | 0.08 | 2 | 96.3 | 0.10 | 0 | 100.0 | 0.14 | 0.09 |
| $F_{64,B}$ | 20 | 0.21 | 54 | 39.2 | 0.25 | 13 | 29.2 | 0.40 | 0.27 |
| $F_{64,B}$ | 30 | 0.15 | 26 | 82.6 | 0.17 | 5 | 64.2 | 0.30 | 0.20 |
| $F_{64,B}$ | 40 | 0.11 | 41 | 52.4 | 0.13 | 5 | 52.8 | 0.21 | 0.14 |
| $F_{64,B}$ | 50 | 0.09 | 16 | 77.3 | 0.11 | 2 | 63.7 | 0.16 | 0.11 |
| $F_{64,B}$ | 60 | 0.08 | 5 | 90.3 | 0.10 | 0 | 100.0 | 0.15 | 0.09 |
| $F_{256,B}$ | 20 | 0.21 | 43 | 60.7 | 0.25 | 5 | 76.4 | 0.39 | 0.27 |
| $F_{256,B}$ | 30 | 0.15 | 24 | 84.0 | 0.17 | 2 | 81.8 | 0.26 | 0.20 |
| $F_{256,B}$ | 40 | 0.11 | 28 | 69.6 | 0.13 | 1 | 82.2 | 0.21 | 0.14 |
| $F_{256,B}$ | 50 | 0.09 | 8 | 89.9 | 0.11 | 1 | 74.1 | 0.17 | 0.11 |
| $F_{256,B}$ | 60 | 0.08 | 5 | 90.0 | 0.10 | 0 | 100.0 | 0.15 | 0.09 |
| $F_{1024,B}$ | 20 | 0.21 | 25 | 94.2 | 0.25 | 4 | 83.4 | 0.40 | 0.26 |
| $F_{1024,B}$ | 30 | 0.15 | 26 | 82.1 | 0.17 | 1 | 93.6 | 0.27 | 0.17 |
| $F_{1024,B}$ | 40 | 0.11 | 18 | 83.1 | 0.13 | 1 | 83.4 | 0.20 | 0.14 |
| $F_{1024,B}$ | 50 | 0.09 | 10 | 87.7 | 0.11 | 0 | 100.0 | 0.16 | 0.10 |
| $F_{1024,B}$ | 60 | 0.08 | 9 | 85.2 | 0.10 | 0 | 100.0 | 0.14 | 0.09 |

* r are the radii of the patches.† V_5^s , V_1^s , and V_0^s delimit the highest 5%, 1%, and the maximum of all V^s values from all patches in all shuffled data.‡ N_i^m is the number of patches in the measured data for which $V^m > V_i^s$, where $i=5$ or 1.# P_i^N is the probability of finding at least N_i^m number of patches with $V^s > V_i^s$ in the randomly shuffled data, where $i=5$ or 1.§ V_0^m is the maximum value of the statistic in the measured data.

Table 4. Results using the Anderson–Darling statistic AD for the *Fermi*/GBM sample.

| Obs. | r^* | $AD_5^{s\dagger}$ | $N_5^{m\dagger}$ | $P_5^{N\#}$ | $AD_1^{s\dagger}$ | $N_1^{m\dagger}$ | $P_1^{N\#}$ | $AD_0^{s\dagger}$ | $AD_0^{m\$}$ |
|--------------|-------|-------------------|------------------|-------------|-------------------|------------------|-------------|-------------------|--------------|
| | (°) | | | (%) | | | (%) | | |
| T_{90} | 20 | 2.51 | 59 | 32.0 | 3.91 | 9 | 48.7 | 11.52 | 5.49 |
| T_{90} | 30 | 2.50 | 70 | 24.3 | 3.91 | 17 | 21.4 | 12.35 | 5.97 |
| T_{90} | 40 | 2.49 | 101 | 10.9 | 3.86 | 18 | 19.7 | 10.91 | 5.15 |
| T_{90} | 50 | 2.50 | 110 | 10.8 | 3.90 | 28 | 11.5 | 11.87 | 6.39 |
| T_{90} | 60 | 2.46 | 116 | 11.6 | 3.84 | 11 | 25.0 | 10.83 | 5.65 |
| S | 20 | 2.51 | 54 | 38.2 | 3.92 | 13 | 28.7 | 11.34 | 5.03 |
| S | 30 | 2.49 | 68 | 23.6 | 3.87 | 16 | 22.5 | 12.10 | 4.60 |
| S | 40 | 2.50 | 60 | 31.5 | 3.92 | 7 | 39.6 | 12.80 | 4.71 |
| S | 50 | 2.51 | 81 | 21.0 | 3.90 | 18 | 19.5 | 11.75 | 5.82 |
| S | 60 | 2.47 | 86 | 19.2 | 3.82 | 15 | 19.5 | 14.62 | 5.07 |
| S_B | 20 | 2.50 | 48 | 49.6 | 3.91 | 7 | 58.5 | 12.72 | 4.51 |
| S_B | 30 | 2.51 | 58 | 34.8 | 3.88 | 12 | 32.7 | 12.10 | 4.61 |
| S_B | 40 | 2.47 | 52 | 40.7 | 3.83 | 5 | 48.9 | 13.51 | 4.30 |
| S_B | 50 | 2.47 | 80 | 21.3 | 3.84 | 16 | 20.0 | 14.03 | 5.55 |
| S_B | 60 | 2.47 | 74 | 24.6 | 3.84 | 9 | 27.5 | 11.48 | 4.75 |
| F_{64} | 20 | 2.50 | 43 | 59.9 | 3.88 | 13 | 30.7 | 12.25 | 5.33 |
| F_{64} | 30 | 2.48 | 54 | 38.2 | 3.86 | 11 | 33.5 | 13.12 | 5.13 |
| F_{64} | 40 | 2.45 | 43 | 49.5 | 3.77 | 5 | 50.1 | 11.33 | 4.83 |
| F_{64} | 50 | 2.47 | 43 | 43.8 | 3.83 | 6 | 37.6 | 10.99 | 4.73 |
| F_{64} | 60 | 2.56 | 42 | 39.3 | 4.02 | 4 | 36.8 | 11.03 | 4.41 |
| F_{256} | 20 | 2.50 | 27 | 90.2 | 3.88 | 4 | 80.4 | 12.51 | 4.26 |
| F_{256} | 30 | 2.51 | 42 | 54.0 | 3.93 | 8 | 43.7 | 13.12 | 4.54 |
| F_{256} | 40 | 2.50 | 47 | 41.7 | 3.90 | 2 | 65.6 | 13.25 | 4.48 |
| F_{256} | 50 | 2.51 | 55 | 35.0 | 3.88 | 5 | 40.8 | 10.75 | 4.65 |
| F_{256} | 60 | 2.48 | 54 | 34.9 | 3.85 | 3 | 45.7 | 12.32 | 4.07 |
| F_{1024} | 20 | 2.49 | 28 | 86.9 | 3.88 | 0 | 100.0 | 11.91 | 3.66 |
| F_{1024} | 30 | 2.49 | 28 | 73.2 | 3.90 | 3 | 68.5 | 10.65 | 4.26 |
| F_{1024} | 40 | 2.46 | 17 | 82.4 | 3.78 | 0 | 100.0 | 11.72 | 3.65 |
| F_{1024} | 50 | 2.52 | 30 | 55.2 | 3.95 | 0 | 100.0 | 12.21 | 3.80 |
| F_{1024} | 60 | 2.48 | 30 | 51.0 | 3.84 | 0 | 100.0 | 11.44 | 3.63 |
| $F_{64,B}$ | 20 | 2.50 | 68 | 19.5 | 3.90 | 19 | 13.6 | 13.81 | 4.94 |
| $F_{64,B}$ | 30 | 2.51 | 82 | 15.5 | 3.90 | 19 | 16.7 | 13.65 | 5.98 |
| $F_{64,B}$ | 40 | 2.49 | 66 | 29.0 | 3.89 | 14 | 25.0 | 11.81 | 6.83 |
| $F_{64,B}$ | 50 | 2.46 | 49 | 39.5 | 3.80 | 3 | 51.5 | 11.31 | 4.85 |
| $F_{64,B}$ | 60 | 2.47 | 29 | 51.5 | 3.83 | 3 | 42.9 | 11.25 | 4.50 |
| $F_{256,B}$ | 20 | 2.51 | 62 | 27.1 | 3.92 | 15 | 23.1 | 13.14 | 5.53 |
| $F_{256,B}$ | 30 | 2.51 | 66 | 27.2 | 3.94 | 16 | 23.4 | 12.42 | 5.44 |
| $F_{256,B}$ | 40 | 2.51 | 43 | 46.7 | 3.92 | 7 | 39.6 | 14.25 | 4.88 |
| $F_{256,B}$ | 50 | 2.46 | 30 | 58.2 | 3.84 | 1 | 66.5 | 12.22 | 3.95 |
| $F_{256,B}$ | 60 | 2.46 | 20 | 61.1 | 3.82 | 1 | 57.0 | 11.20 | 4.08 |
| $F_{1024,B}$ | 20 | 2.48 | 45 | 55.9 | 3.84 | 4 | 76.1 | 11.20 | 4.14 |
| $F_{1024,B}$ | 30 | 2.50 | 42 | 54.2 | 3.90 | 5 | 56.9 | 11.23 | 4.23 |
| $F_{1024,B}$ | 40 | 2.48 | 14 | 85.7 | 3.86 | 0 | 100.0 | 10.22 | 3.31 |
| $F_{1024,B}$ | 50 | 2.51 | 16 | 73.3 | 3.93 | 0 | 100.0 | 12.33 | 3.55 |
| $F_{1024,B}$ | 60 | 2.49 | 9 | 76.4 | 3.86 | 0 | 100.0 | 13.27 | 3.40 |

* r are the radii of the patches.† AD_5^s , AD_1^s , and AD_0^s delimit the highest 5%, 1%, and the maximum of all AD^s values from all patches in all shuffled data.‡ N_i^m is the number of patches in the measured data for which $AD_i^m > AD_i^s$, where $i=5$ or 1.# P_i^N is the probability of finding at least N_i^m number of patches with $AD^s > AD_i^s$ in the randomly shuffled data, where $i=5$ or 1.§ AD_0^m is the maximum value of the statistic in the measured data.**Table 5.** Results using the χ^2 statistic for the *Fermi*/GBM sample.

| Obs. | r^* | $\chi_5^{2s\dagger}$ | $N_5^{m\dagger}$ | $P_5^{N\#}$ | $\chi_1^{2s\dagger}$ | $N_1^{m\dagger}$ | $P_1^{N\#}$ | $\chi_0^{2s\dagger}$ | $\chi_0^{2m\$}$ |
|--------------|-------|----------------------|------------------|-------------|----------------------|------------------|-------------|----------------------|-----------------|
| | (°) | | | (%) | | | (%) | | |
| T_{90} | 20 | 20.49 | 32 | 95.7 | 42.28 | 13 | 32.1 | 105.65 | 50.59 |
| T_{90} | 30 | 20.70 | 69 | 16.9 | 27.35 | 17 | 21.9 | 72.21 | 32.31 |
| T_{90} | 40 | 17.99 | 77 | 18.5 | 23.39 | 23 | 14.0 | 64.98 | 28.85 |
| T_{90} | 50 | 17.04 | 85 | 17.0 | 21.97 | 10 | 31.6 | 47.40 | 26.14 |
| T_{90} | 60 | 16.66 | 56 | 34.6 | 21.22 | 4 | 46.6 | 40.71 | 23.59 |
| S | 20 | 18.12 | 34 | 92.8 | 41.07 | 2 | 84.0 | 81.36 | 46.37 |
| S | 30 | 19.40 | 22 | 93.7 | 25.50 | 5 | 61.7 | 52.10 | 26.90 |
| S | 40 | 16.60 | 11 | 93.7 | 21.71 | 0 | 100.0 | 63.67 | 21.22 |
| S | 50 | 15.61 | 6 | 92.9 | 20.28 | 0 | 100.0 | 44.25 | 17.27 |
| S | 60 | 15.37 | 5 | 89.3 | 19.88 | 0 | 100.0 | 44.48 | 18.41 |
| S_B | 20 | 33.68 | 42 | 79.1 | 45.10 | 6 | 62.5 | 109.56 | 48.03 |
| S_B | 30 | 21.95 | 43 | 62.1 | 28.85 | 2 | 73.2 | 67.15 | 31.43 |
| S_B | 40 | 18.59 | 5 | 98.1 | 24.02 | 0 | 100.0 | 49.99 | 21.87 |
| S_B | 50 | 17.17 | 3 | 97.2 | 21.96 | 0 | 100.0 | 42.69 | 19.36 |
| S_B | 60 | 16.54 | 6 | 87.0 | 21.00 | 0 | 100.0 | 57.53 | 18.05 |
| F_{64} | 20 | 33.16 | 31 | 94.1 | 44.06 | 5 | 66.1 | 108.67 | 57.29 |
| F_{64} | 30 | 20.97 | 22 | 89.5 | 28.75 | 1 | 75.9 | 88.29 | 30.85 |
| F_{64} | 40 | 17.50 | 14 | 87.2 | 23.15 | 0 | 100.0 | 48.12 | 20.18 |
| F_{64} | 50 | 15.74 | 5 | 94.1 | 20.39 | 0 | 100.0 | 41.88 | 17.77 |
| F_{64} | 60 | 15.02 | 21 | 67.4 | 19.42 | 0 | 100.0 | 37.39 | 18.95 |
| F_{256} | 20 | 25.19 | 39 | 81.0 | 43.65 | 2 | 80.6 | 133.79 | 47.40 |
| F_{256} | 30 | 21.30 | 22 | 89.3 | 29.75 | 0 | 100.0 | 78.30 | 29.64 |
| F_{256} | 40 | 18.59 | 19 | 81.6 | 24.82 | 3 | 55.5 | 59.53 | 27.47 |
| F_{256} | 50 | 17.35 | 20 | 75.0 | 22.45 | 1 | 71.6 | 44.54 | 22.99 |
| F_{256} | 60 | 16.76 | 19 | 68.0 | 21.40 | 0 | 100.0 | 38.42 | 20.94 |
| F_{1024} | 20 | 33.70 | 37 | 87.8 | 45.40 | 14 | 28.5 | 114.66 | 63.17 |
| F_{1024} | 30 | 22.22 | 32 | 79.9 | 29.80 | 2 | 70.3 | 63.86 | 30.60 |
| F_{1024} | 40 | 18.76 | 18 | 83.2 | 24.77 | 0 | 100.0 | 53.46 | 21.07 |
| F_{1024} | 50 | 17.21 | 1 | 97.7 | 22.17 | 0 | 100.0 | 46.48 | 17.58 |
| F_{1024} | 60 | 16.48 | 12 | 79.1 | 21.05 | 1 | 65.4 | 39.61 | 24.08 |
| $F_{64,B}$ | 20 | 36.67 | 28 | 92.6 | 47.23 | 4 | 70.7 | 127.40 | 52.94 |
| $F_{64,B}$ | 30 | 23.16 | 10 | 98.4 | 32.45 | 1 | 77.5 | 63.47 | 33.03 |
| $F_{64,B}$ | 40 | 19.53 | 16 | 88.0 | 25.52 | 0 | 100.0 | 52.68 | 23.94 |
| $F_{64,B}$ | 50 | 17.23 | 10 | 88.5 | 22.08 | 0 | 100.0 | 45.86 | 19.08 |
| $F_{64,B}$ | 60 | 16.31 | 13 | 78.1 | 20.75 | 0 | 100.0 | 39.04 | 18.13 |
| $F_{256,B}$ | 20 | 36.94 | 39 | 76.8 | 47.83 | 7 | 56.1 | 137.68 | 53.18 |
| $F_{256,B}$ | 30 | 23.16 | 19 | 91.0 | 33.37 | 0 | 100.0 | 84.43 | 32.85 |
| $F_{256,B}$ | 40 | 19.60 | 15 | 87.9 | 25.69 | 0 | 100.0 | 51.59 | 24.00 |
| $F_{256,B}$ | 50 | 17.31 | 4 | 94.8 | 22.29 | 0 | 100.0 | 48.37 | 18.07 |
| $F_{256,B}$ | 60 | 16.27 | 11 | 81.8 | 20.75 | 0 | 100.0 | 42.27 | 19.08 |
| $F_{1024,B}$ | 20 | 37.92 | 41 | 69.5 | 48.09 | 0 | 100.0 | 148.32 | 47.15 |
| $F_{1024,B}$ | 30 | 23.51 | 13 | 96.4 | 34.11 | 0 | 100.0 | 70.19 | 28.01 |
| $F_{1024,B}$ | 40 | 19.95 | 18 | 85.2 | 25.87 | 0 | 100.0 | 67.27 | 23.59 |
| $F_{1024,B}$ | 50 | 17.32 | 22 | 73.2 | 22.07 | 5 | 45.0 | 44.24 | 23.94 |
| $F_{1024,B}$ | 60 | 16.00 | 31 | 55.6 | 20.05 | 4 | 45.2 | 41.04 | 20.88 |

* r are the radii of the patches.† χ_5^{2s} , χ_1^{2s} , and χ_0^{2s} delimit the highest 5%, 1%, and the maximum of all χ^{2s} values from all patches in all shuffled data.‡ N_i^m is the number of patches in the measured data for which $\chi^{2m} > \chi_i^{2s}$, where $i=5$ or 1.# P_i^N is the probability of finding at least N_i^m number of patches with $\chi^{2s} > \chi_i^{2s}$ in the randomly shuffled data, where $i=5$ or 1.§ χ_0^{2m} is the maximum value of the statistic in the measured data.

Table 6. Results using the Kolmogorov–Smirnov statistic D for the *CGRO/BATSE* sample.

| Obs. | r^* ($^\circ$) | $D_5^{s\dagger}$ | $N_5^{m\dagger}$ | $P_5^{N\#}$ (%) | $D_1^{s\dagger}$ | $N_1^{m\dagger}$ | $P_1^{N\#}$ (%) | $D_0^{s\dagger}$ | $D_0^{m\$}$ |
|--------------|-----------------------|------------------|------------------|--------------------|------------------|------------------|--------------------|------------------|-------------|
| T_{90} | 20 | 0.18 | 48 | 49.4 | 0.21 | 3 | 85.1 | 0.44 | 0.25 |
| T_{90} | 30 | 0.12 | 29 | 77.1 | 0.14 | 8 | 45.2 | 0.23 | 0.17 |
| T_{90} | 40 | 0.09 | 23 | 74.4 | 0.11 | 2 | 71.6 | 0.17 | 0.12 |
| T_{90} | 50 | 0.08 | 28 | 60.6 | 0.09 | 5 | 44.0 | 0.17 | 0.10 |
| T_{90} | 60 | 0.07 | 11 | 74.1 | 0.08 | 0 | 100.0 | 0.13 | 0.07 |
| S_1 | 20 | 0.17 | 60 | 27.2 | 0.21 | 12 | 33.8 | 0.36 | 0.27 |
| S_1 | 30 | 0.12 | 66 | 26.8 | 0.14 | 8 | 46.1 | 0.25 | 0.16 |
| S_1 | 40 | 0.09 | 39 | 53.1 | 0.11 | 6 | 47.9 | 0.17 | 0.12 |
| S_1 | 50 | 0.08 | 32 | 54.9 | 0.09 | 5 | 42.2 | 0.15 | 0.10 |
| S_1 | 60 | 0.07 | 13 | 72.5 | 0.08 | 2 | 52.4 | 0.13 | 0.09 |
| S_2 | 20 | 0.17 | 34 | 79.0 | 0.21 | 8 | 54.9 | 0.38 | 0.24 |
| S_2 | 30 | 0.12 | 26 | 81.6 | 0.14 | 4 | 68.7 | 0.23 | 0.16 |
| S_2 | 40 | 0.09 | 14 | 86.6 | 0.11 | 1 | 79.3 | 0.19 | 0.11 |
| S_2 | 50 | 0.08 | 7 | 89.7 | 0.09 | 0 | 100.0 | 0.15 | 0.08 |
| S_2 | 60 | 0.07 | 8 | 84.1 | 0.08 | 0 | 100.0 | 0.13 | 0.08 |
| S_3 | 20 | 0.17 | 35 | 78.6 | 0.21 | 6 | 68.6 | 0.35 | 0.24 |
| S_3 | 30 | 0.12 | 27 | 79.1 | 0.14 | 1 | 88.7 | 0.23 | 0.16 |
| S_3 | 40 | 0.09 | 13 | 86.8 | 0.11 | 0 | 100.0 | 0.19 | 0.11 |
| S_3 | 50 | 0.08 | 8 | 87.0 | 0.09 | 0 | 100.0 | 0.15 | 0.09 |
| S_3 | 60 | 0.07 | 5 | 88.9 | 0.08 | 0 | 100.0 | 0.13 | 0.08 |
| S_4 | 20 | 0.19 | 34 | 80.8 | 0.23 | 7 | 60.7 | 0.39 | 0.28 |
| S_4 | 30 | 0.13 | 44 | 50.8 | 0.16 | 7 | 49.0 | 0.27 | 0.18 |
| S_4 | 40 | 0.10 | 25 | 71.8 | 0.12 | 1 | 80.5 | 0.20 | 0.12 |
| S_4 | 50 | 0.08 | 10 | 86.5 | 0.10 | 1 | 73.5 | 0.16 | 0.11 |
| S_4 | 60 | 0.07 | 22 | 63.2 | 0.09 | 0 | 100.0 | 0.16 | 0.08 |
| $F_{64,B}$ | 20 | 0.17 | 27 | 88.7 | 0.21 | 1 | 97.4 | 0.36 | 0.21 |
| $F_{64,B}$ | 30 | 0.12 | 23 | 84.6 | 0.14 | 3 | 73.1 | 0.24 | 0.15 |
| $F_{64,B}$ | 40 | 0.09 | 26 | 69.3 | 0.11 | 1 | 77.9 | 0.18 | 0.11 |
| $F_{64,B}$ | 50 | 0.08 | 1 | 98.7 | 0.09 | 0 | 100.0 | 0.17 | 0.08 |
| $F_{64,B}$ | 60 | 0.07 | 3 | 93.2 | 0.08 | 0 | 100.0 | 0.13 | 0.07 |
| $F_{256,B}$ | 20 | 0.17 | 14 | 99.6 | 0.21 | 0 | 100.0 | 0.44 | 0.21 |
| $F_{256,B}$ | 30 | 0.12 | 20 | 87.6 | 0.14 | 5 | 59.2 | 0.23 | 0.15 |
| $F_{256,B}$ | 40 | 0.09 | 17 | 81.9 | 0.11 | 5 | 52.3 | 0.19 | 0.12 |
| $F_{256,B}$ | 50 | 0.08 | 1 | 98.6 | 0.09 | 0 | 100.0 | 0.17 | 0.08 |
| $F_{256,B}$ | 60 | 0.07 | 3 | 92.6 | 0.08 | 0 | 100.0 | 0.13 | 0.07 |
| $F_{1024,B}$ | 20 | 0.17 | 24 | 94.0 | 0.21 | 3 | 86.6 | 0.36 | 0.22 |
| $F_{1024,B}$ | 30 | 0.12 | 16 | 93.3 | 0.14 | 3 | 73.3 | 0.23 | 0.16 |
| $F_{1024,B}$ | 40 | 0.09 | 29 | 65.8 | 0.11 | 4 | 54.8 | 0.19 | 0.12 |
| $F_{1024,B}$ | 50 | 0.08 | 5 | 92.2 | 0.09 | 0 | 100.0 | 0.14 | 0.08 |
| $F_{1024,B}$ | 60 | 0.07 | 7 | 87.4 | 0.08 | 0 | 100.0 | 0.13 | 0.08 |

* r are the radii of the patches.

† D_5^s , D_1^s , and D_0^s delimit the highest 5%, 1%, and the maximum of all D^s values from all patches in all shuffled data.

‡ N_i^m is the number of patches in the measured data for which $D^m > D_i^s$, where $i=5$ or 1.

P_i^N is the probability of finding at least N_i^m number of patches with $D^s > D_i^s$ in the randomly shuffled data, where $i=5$ or 1.

§ D_0^m is the maximum value of the statistic in the measured data.

Table 7. Results using the Kuiper statistic V for the *CGRO/BATSE* sample.

| Obs. | r^* ($^\circ$) | $V_5^{s\dagger}$ | $N_5^{m\dagger}$ | $P_5^{N\#}$ (%) | $V_1^{s\dagger}$ | $N_1^{m\dagger}$ | $P_1^{N\#}$ (%) | $V_0^{s\dagger}$ | $V_0^{m\$}$ |
|--------------|-----------------------|------------------|------------------|--------------------|------------------|------------------|--------------------|------------------|-------------|
| T_{90} | 20 | 0.23 | 26 | 92.9 | 0.26 | 3 | 89.2 | 0.49 | 0.28 |
| T_{90} | 30 | 0.15 | 13 | 96.8 | 0.18 | 1 | 92.7 | 0.27 | 0.18 |
| T_{90} | 40 | 0.12 | 1 | 99.6 | 0.14 | 0 | 100.0 | 0.21 | 0.12 |
| T_{90} | 50 | 0.10 | 1 | 98.5 | 0.12 | 0 | 100.0 | 0.17 | 0.10 |
| T_{90} | 60 | 0.09 | 3 | 93.0 | 0.10 | 0 | 100.0 | 0.15 | 0.10 |
| S_1 | 20 | 0.22 | 60 | 25.8 | 0.26 | 11 | 38.6 | 0.41 | 0.31 |
| S_1 | 30 | 0.15 | 59 | 31.9 | 0.17 | 10 | 38.9 | 0.26 | 0.20 |
| S_1 | 40 | 0.12 | 32 | 65.2 | 0.14 | 1 | 82.5 | 0.20 | 0.14 |
| S_1 | 50 | 0.10 | 23 | 68.0 | 0.11 | 0 | 100.0 | 0.18 | 0.11 |
| S_1 | 60 | 0.09 | 7 | 86.4 | 0.10 | 0 | 100.0 | 0.15 | 0.10 |
| S_2 | 20 | 0.22 | 34 | 80.6 | 0.26 | 12 | 33.8 | 0.45 | 0.29 |
| S_2 | 30 | 0.15 | 15 | 96.3 | 0.17 | 1 | 93.1 | 0.26 | 0.18 |
| S_2 | 40 | 0.12 | 16 | 87.7 | 0.13 | 1 | 84.0 | 0.20 | 0.14 |
| S_2 | 50 | 0.10 | 5 | 93.6 | 0.11 | 0 | 100.0 | 0.18 | 0.11 |
| S_2 | 60 | 0.09 | 1 | 96.9 | 0.10 | 0 | 100.0 | 0.14 | 0.09 |
| S_3 | 20 | 0.22 | 49 | 49.5 | 0.25 | 7 | 65.2 | 0.39 | 0.27 |
| S_3 | 30 | 0.15 | 47 | 48.8 | 0.17 | 7 | 52.5 | 0.30 | 0.19 |
| S_3 | 40 | 0.12 | 30 | 66.1 | 0.13 | 1 | 82.5 | 0.20 | 0.14 |
| S_3 | 50 | 0.10 | 23 | 69.6 | 0.11 | 1 | 75.6 | 0.16 | 0.11 |
| S_3 | 60 | 0.09 | 8 | 83.8 | 0.10 | 0 | 100.0 | 0.14 | 0.09 |
| S_4 | 20 | 0.24 | 42 | 63.6 | 0.28 | 10 | 43.5 | 0.45 | 0.35 |
| S_4 | 30 | 0.17 | 48 | 48.4 | 0.19 | 4 | 71.3 | 0.33 | 0.20 |
| S_4 | 40 | 0.13 | 36 | 60.0 | 0.15 | 0 | 100.0 | 0.21 | 0.15 |
| S_4 | 50 | 0.11 | 57 | 33.0 | 0.12 | 2 | 65.8 | 0.20 | 0.13 |
| S_4 | 60 | 0.09 | 74 | 24.5 | 0.11 | 3 | 52.2 | 0.17 | 0.11 |
| $F_{64,B}$ | 20 | 0.22 | 37 | 73.8 | 0.25 | 4 | 82.2 | 0.41 | 0.30 |
| $F_{64,B}$ | 30 | 0.15 | 37 | 64.7 | 0.17 | 6 | 58.3 | 0.28 | 0.19 |
| $F_{64,B}$ | 40 | 0.12 | 25 | 74.2 | 0.13 | 7 | 45.9 | 0.20 | 0.16 |
| $F_{64,B}$ | 50 | 0.10 | 23 | 67.0 | 0.11 | 2 | 62.9 | 0.17 | 0.12 |
| $F_{64,B}$ | 60 | 0.09 | 6 | 88.0 | 0.10 | 0 | 100.0 | 0.15 | 0.10 |
| $F_{256,B}$ | 20 | 0.22 | 17 | 98.5 | 0.25 | 4 | 82.9 | 0.44 | 0.28 |
| $F_{256,B}$ | 30 | 0.15 | 25 | 83.6 | 0.17 | 5 | 64.0 | 0.26 | 0.19 |
| $F_{256,B}$ | 40 | 0.12 | 37 | 56.4 | 0.13 | 10 | 34.2 | 0.20 | 0.15 |
| $F_{256,B}$ | 50 | 0.10 | 21 | 71.9 | 0.11 | 1 | 74.2 | 0.17 | 0.11 |
| $F_{256,B}$ | 60 | 0.09 | 5 | 89.8 | 0.10 | 0 | 100.0 | 0.14 | 0.10 |
| $F_{1024,B}$ | 20 | 0.22 | 35 | 79.7 | 0.25 | 4 | 81.9 | 0.39 | 0.26 |
| $F_{1024,B}$ | 30 | 0.15 | 19 | 92.8 | 0.17 | 0 | 100.0 | 0.26 | 0.17 |
| $F_{1024,B}$ | 40 | 0.12 | 35 | 58.1 | 0.13 | 3 | 63.1 | 0.20 | 0.14 |
| $F_{1024,B}$ | 50 | 0.10 | 10 | 86.1 | 0.11 | 0 | 100.0 | 0.16 | 0.10 |
| $F_{1024,B}$ | 60 | 0.09 | 3 | 94.7 | 0.10 | 0 | 100.0 | 0.14 | 0.09 |

* r are the radii of the patches.

† V_5^s , V_1^s , and V_0^s delimit the highest 5%, 1%, and the maximum of all V^s values from all patches in all shuffled data.

‡ N_i^m is the number of patches in the measured data for which $V^m > V_i^s$, where $i=5$ or 1.

P_i^N is the probability of finding at least N_i^m number of patches with $V^s > V_i^s$ in the randomly shuffled data, where $i=5$ or 1.

§ V_0^m is the maximum value of the statistic in the measured data.

Table 8. Results using the Anderson–Darling statistic AD for the *CGRO/BATSE* sample.

| Obs. | r^* | $AD_5^{s\dagger}$ | $N_5^{m\dagger}$ | $P_5^{N\#}$ | $AD_1^{s\dagger}$ | $N_1^{m\dagger}$ | $P_1^{N\#}$ | $AD_0^{s\dagger}$ | $AD_0^{m\$}$ |
|--------------|-------|-------------------|------------------|-------------|-------------------|------------------|-------------|-------------------|--------------|
| | (°) | | | (%) | | | (%) | | |
| T_{90} | 20 | 2.51 | 49 | 47.2 | 3.90 | 15 | 23.8 | 11.95 | 5.34 |
| T_{90} | 30 | 2.48 | 53 | 40.0 | 3.85 | 10 | 37.8 | 13.49 | 6.08 |
| T_{90} | 40 | 2.52 | 62 | 30.3 | 3.91 | 12 | 26.9 | 12.31 | 6.71 |
| T_{90} | 50 | 2.49 | 52 | 36.1 | 3.84 | 19 | 18.1 | 11.69 | 5.66 |
| T_{90} | 60 | 2.50 | 48 | 37.7 | 3.89 | 2 | 48.4 | 14.28 | 4.01 |
| S_1 | 20 | 2.49 | 42 | 62.5 | 3.87 | 10 | 43.5 | 11.71 | 5.92 |
| S_1 | 30 | 2.49 | 64 | 28.2 | 3.88 | 6 | 55.3 | 11.19 | 4.92 |
| S_1 | 40 | 2.48 | 52 | 38.3 | 3.86 | 15 | 24.2 | 11.57 | 4.97 |
| S_1 | 50 | 2.46 | 44 | 41.3 | 3.86 | 4 | 43.2 | 11.57 | 4.69 |
| S_1 | 60 | 2.46 | 24 | 56.8 | 3.84 | 0 | 100.0 | 11.78 | 3.83 |
| S_2 | 20 | 2.50 | 28 | 85.2 | 3.90 | 3 | 84.3 | 12.37 | 4.33 |
| S_2 | 30 | 2.48 | 24 | 80.6 | 3.86 | 2 | 76.9 | 12.41 | 4.38 |
| S_2 | 40 | 2.51 | 19 | 77.3 | 3.94 | 1 | 72.8 | 12.66 | 3.96 |
| S_2 | 50 | 2.56 | 10 | 80.8 | 4.03 | 0 | 100.0 | 13.54 | 3.94 |
| S_2 | 60 | 2.49 | 7 | 80.5 | 3.90 | 0 | 100.0 | 11.17 | 3.64 |
| S_3 | 20 | 2.49 | 24 | 92.3 | 3.85 | 0 | 100.0 | 12.22 | 3.68 |
| S_3 | 30 | 2.50 | 13 | 94.6 | 3.89 | 2 | 76.7 | 11.91 | 4.26 |
| S_3 | 40 | 2.50 | 15 | 82.7 | 3.89 | 0 | 100.0 | 11.78 | 3.55 |
| S_3 | 50 | 2.51 | 4 | 91.4 | 3.94 | 0 | 100.0 | 10.93 | 3.16 |
| S_3 | 60 | 2.51 | 6 | 83.4 | 3.91 | 0 | 100.0 | 11.62 | 3.23 |
| S_4 | 20 | 2.48 | 39 | 69.2 | 3.85 | 8 | 52.0 | 12.05 | 5.14 |
| S_4 | 30 | 2.51 | 30 | 70.1 | 3.89 | 2 | 77.6 | 14.17 | 4.97 |
| S_4 | 40 | 2.51 | 13 | 86.6 | 3.93 | 0 | 100.0 | 12.05 | 3.40 |
| S_4 | 50 | 2.46 | 22 | 66.4 | 3.77 | 2 | 57.9 | 12.19 | 5.63 |
| S_4 | 60 | 2.47 | 30 | 51.3 | 3.82 | 3 | 44.0 | 19.49 | 4.57 |
| $F_{64,B}$ | 20 | 2.48 | 19 | 95.9 | 3.84 | 5 | 71.7 | 12.79 | 5.30 |
| $F_{64,B}$ | 30 | 2.50 | 17 | 89.0 | 3.89 | 1 | 85.5 | 11.76 | 4.80 |
| $F_{64,B}$ | 40 | 2.50 | 10 | 88.7 | 3.89 | 0 | 100.0 | 12.81 | 3.43 |
| $F_{64,B}$ | 50 | 2.50 | 2 | 96.3 | 3.88 | 0 | 100.0 | 15.12 | 3.31 |
| $F_{64,B}$ | 60 | 2.45 | 0 | 100.0 | 3.82 | 0 | 100.0 | 13.20 | 2.17 |
| $F_{256,B}$ | 20 | 2.48 | 14 | 98.6 | 3.86 | 1 | 97.5 | 12.68 | 4.28 |
| $F_{256,B}$ | 30 | 2.46 | 12 | 94.2 | 3.86 | 1 | 87.3 | 11.76 | 3.86 |
| $F_{256,B}$ | 40 | 2.52 | 8 | 91.2 | 3.93 | 0 | 100.0 | 12.07 | 3.34 |
| $F_{256,B}$ | 50 | 2.46 | 2 | 95.7 | 3.83 | 0 | 100.0 | 12.62 | 2.64 |
| $F_{256,B}$ | 60 | 2.53 | 0 | 100.0 | 3.94 | 0 | 100.0 | 10.88 | 2.38 |
| $F_{1024,B}$ | 20 | 2.48 | 20 | 95.9 | 3.87 | 2 | 91.3 | 12.27 | 4.40 |
| $F_{1024,B}$ | 30 | 2.49 | 9 | 97.5 | 3.85 | 0 | 100.0 | 10.83 | 3.60 |
| $F_{1024,B}$ | 40 | 2.49 | 8 | 93.9 | 3.88 | 0 | 100.0 | 10.95 | 3.60 |
| $F_{1024,B}$ | 50 | 2.51 | 0 | 100.0 | 3.87 | 0 | 100.0 | 10.13 | 2.42 |
| $F_{1024,B}$ | 60 | 2.45 | 4 | 87.2 | 3.76 | 0 | 100.0 | 10.44 | 2.83 |

* r are the radii of the patches.

† AD_5^s , AD_1^s , and AD_0^s delimit the highest 5 %, 1 %, and the maximum of all AD^s values from all patches in all shuffled data.

‡ N_i^m is the number of patches in the measured data for which $AD_i^m > AD_i^s$, where $i=5$ or 1.

P_i^N is the probability of finding at least N_i^m number of patches with $AD^s > AD_i^s$ in the randomly shuffled data, where $i=5$ or 1.

§ AD_0^m is the maximum value of the statistic in the measured data.

Table 9. Results using the χ^2 statistic for the *CGRO/BATSE* sample.

| Obs. | r^* | $\chi_5^{2s\dagger}$ | $N_5^{m\dagger}$ | $P_5^{N\#}$ | $\chi_1^{2s\dagger}$ | $N_1^{m\dagger}$ | $P_1^{N\#}$ | $\chi_0^{2s\dagger}$ | $\chi_0^{2m\$}$ |
|--------------|-------|----------------------|------------------|-------------|----------------------|------------------|-------------|----------------------|-----------------|
| | (°) | | | (%) | | | (%) | | |
| T_{90} | 20 | 19.96 | 49 | 50.2 | 42.36 | 2 | 85.1 | 88.46 | 47.29 |
| T_{90} | 30 | 20.51 | 39 | 70.1 | 26.81 | 0 | 100.0 | 61.83 | 26.57 |
| T_{90} | 40 | 17.96 | 32 | 67.7 | 23.17 | 2 | 72.8 | 51.97 | 29.02 |
| T_{90} | 50 | 16.91 | 55 | 36.6 | 21.72 | 9 | 35.8 | 51.18 | 26.94 |
| T_{90} | 60 | 16.84 | 53 | 37.6 | 21.54 | 11 | 28.1 | 44.06 | 26.19 |
| S_1 | 20 | 33.57 | 64 | 10.4 | 45.69 | 28 | 4.1 | 116.00 | 60.63 |
| S_1 | 30 | 22.14 | 45 | 57.0 | 29.06 | 1 | 83.7 | 65.88 | 37.37 |
| S_1 | 40 | 18.65 | 49 | 45.6 | 24.18 | 1 | 75.7 | 56.58 | 25.45 |
| S_1 | 50 | 17.25 | 22 | 72.6 | 22.11 | 2 | 63.9 | 44.27 | 23.50 |
| S_1 | 60 | 16.35 | 14 | 75.2 | 20.83 | 0 | 100.0 | 42.01 | 19.38 |
| S_2 | 20 | 19.84 | 51 | 43.9 | 42.51 | 7 | 57.8 | 95.91 | 52.74 |
| S_2 | 30 | 20.55 | 51 | 47.4 | 26.87 | 18 | 20.0 | 66.60 | 38.67 |
| S_2 | 40 | 17.90 | 34 | 64.8 | 23.25 | 1 | 79.6 | 56.88 | 24.04 |
| S_2 | 50 | 17.18 | 11 | 85.7 | 22.07 | 2 | 61.9 | 44.57 | 22.89 |
| S_2 | 60 | 16.80 | 6 | 89.0 | 21.46 | 0 | 100.0 | 44.25 | 20.78 |
| S_3 | 20 | 34.22 | 44 | 70.1 | 45.80 | 7 | 56.0 | 108.51 | 54.62 |
| S_3 | 30 | 22.16 | 37 | 72.2 | 29.74 | 0 | 100.0 | 68.47 | 27.49 |
| S_3 | 40 | 18.76 | 29 | 70.6 | 24.42 | 5 | 50.1 | 57.26 | 27.34 |
| S_3 | 50 | 17.04 | 18 | 77.1 | 21.85 | 1 | 71.3 | 54.06 | 22.00 |
| S_3 | 60 | 16.60 | 7 | 85.7 | 21.32 | 0 | 100.0 | 46.89 | 18.89 |
| S_4 | 20 | 25.57 | 54 | 36.6 | 43.32 | 12 | 36.5 | 130.70 | 52.48 |
| S_4 | 30 | 21.40 | 33 | 77.1 | 30.03 | 0 | 100.0 | 87.01 | 28.08 |
| S_4 | 40 | 18.47 | 20 | 81.3 | 24.71 | 5 | 51.2 | 63.35 | 28.37 |
| S_4 | 50 | 17.11 | 11 | 87.3 | 22.09 | 1 | 72.2 | 44.20 | 23.15 |
| S_4 | 60 | 16.48 | 8 | 85.8 | 21.04 | 0 | 100.0 | 45.55 | 18.27 |
| $F_{64,B}$ | 20 | 24.26 | 46 | 61.0 | 42.58 | 17 | 20.7 | 127.07 | 53.21 |
| $F_{64,B}$ | 30 | 20.69 | 38 | 70.1 | 28.55 | 6 | 48.0 | 64.22 | 38.23 |
| $F_{64,B}$ | 40 | 18.47 | 4 | 97.6 | 24.40 | 0 | 100.0 | 51.31 | 20.00 |
| $F_{64,B}$ | 50 | 17.19 | 1 | 99.5 | 22.00 | 0 | 100.0 | 46.10 | 18.04 |
| $F_{64,B}$ | 60 | 16.69 | 2 | 95.0 | 21.35 | 0 | 100.0 | 42.09 | 17.15 |
| $F_{256,B}$ | 20 | 33.23 | 64 | 9.6 | 45.06 | 14 | 27.8 | 109.81 | 50.47 |
| $F_{256,B}$ | 30 | 21.96 | 56 | 38.8 | 28.81 | 9 | 38.8 | 64.38 | 41.89 |
| $F_{256,B}$ | 40 | 18.62 | 29 | 71.1 | 24.01 | 4 | 59.2 | 49.85 | 27.44 |
| $F_{256,B}$ | 50 | 17.02 | 15 | 82.3 | 21.67 | 0 | 100.0 | 45.59 | 20.03 |
| $F_{256,B}$ | 60 | 16.51 | 6 | 88.6 | 21.01 | 0 | 100.0 | 41.40 | 20.44 |
| $F_{1024,B}$ | 20 | 24.35 | 39 | 82.8 | 42.74 | 8 | 52.3 | 116.66 | 48.44 |
| $F_{1024,B}$ | 30 | 20.93 | 37 | 70.7 | 29.22 | 4 | 54.1 | 67.22 | 33.24 |
| $F_{1024,B}$ | 40 | 18.42 | 32 | 65.6 | 24.26 | 2 | 66.1 | 48.56 | 25.71 |
| $F_{1024,B}$ | 50 | 17.17 | 29 | 64.5 | 21.98 | 6 | 44.6 | 50.16 | 24.46 |
| $F_{1024,B}$ | 60 | 16.72 | 33 | 53.0 | 21.18 | 0 | 100.0 | 40.57 | 20.05 |

* r are the radii of the patches.

† χ_5^{2s} , χ_1^{2s} , and χ_0^{2s} delimit the highest 5 %, 1 %, and the maximum of all χ^{2s} values from all patches in all shuffled data.

‡ N_i^m is the number of patches in the measured data for which $\chi^{2m} > \chi_i^{2s}$, where $i=5$ or 1.

P_i^N is the probability of finding at least N_i^m number of patches with $\chi^{2s} > \chi_i^{2s}$ in the randomly shuffled data, where $i=5$ or 1. The case with $P_i^N \leq 5\%$ is emphasized in boldface.

§ χ_0^{2m} is the maximum value of the statistic in the measured data.

Table 10. Results using the Kolmogorov–Smirnov statistic D for the *Swift*/BAT sample.

| Obs. | r | D_5^s | N_5^m | P_5^N (%) | D_1^s | N_1^m | P_1^N (%) | D_0^s | D_0^m |
|----------|-----|---------|---------|----------------|---------|---------|----------------|---------|---------|
| T_{90} | 20 | 0.23 | 50 | 45.8 | 0.29 | 11 | 38.1 | 0.50 | 0.34 |
| T_{90} | 30 | 0.16 | 68 | 22.5 | 0.19 | 12 | 32.3 | 0.32 | 0.22 |
| T_{90} | 40 | 0.12 | 116 | 6.1 | 0.15 | 19 | 18.3 | 0.24 | 0.18 |
| T_{90} | 50 | 0.10 | 163 | 2.9 | 0.12 | 55 | 2.9 | 0.19 | 0.16 |
| T_{90} | 60 | 0.09 | 178 | 4.0 | 0.11 | 56 | 3.6 | 0.17 | 0.14 |
| S_1 | 20 | 0.24 | 32 | 83.5 | 0.29 | 6 | 68.1 | 0.50 | 0.33 |
| S_1 | 30 | 0.16 | 7 | 98.5 | 0.19 | 0 | 100.0 | 0.32 | 0.18 |
| S_1 | 40 | 0.12 | 14 | 86.0 | 0.15 | 0 | 100.0 | 0.24 | 0.15 |
| S_1 | 50 | 0.10 | 6 | 91.2 | 0.12 | 0 | 100.0 | 0.21 | 0.12 |
| S_1 | 60 | 0.09 | 1 | 96.8 | 0.11 | 0 | 100.0 | 0.18 | 0.09 |
| S_2 | 20 | 0.24 | 20 | 96.8 | 0.29 | 5 | 76.6 | 0.54 | 0.36 |
| S_2 | 30 | 0.16 | 6 | 99.8 | 0.19 | 0 | 100.0 | 0.33 | 0.18 |
| S_2 | 40 | 0.12 | 7 | 96.0 | 0.15 | 0 | 100.0 | 0.25 | 0.14 |
| S_2 | 50 | 0.10 | 1 | 98.4 | 0.12 | 0 | 100.0 | 0.23 | 0.10 |
| S_2 | 60 | 0.09 | 1 | 95.3 | 0.11 | 0 | 100.0 | 0.18 | 0.09 |
| S_3 | 20 | 0.23 | 28 | 91.3 | 0.29 | 4 | 84.0 | 0.55 | 0.35 |
| S_3 | 30 | 0.16 | 10 | 98.2 | 0.19 | 1 | 91.1 | 0.32 | 0.22 |
| S_3 | 40 | 0.12 | 10 | 93.4 | 0.15 | 0 | 100.0 | 0.24 | 0.14 |
| S_3 | 50 | 0.10 | 3 | 96.8 | 0.12 | 0 | 100.0 | 0.21 | 0.10 |
| S_3 | 60 | 0.09 | 2 | 95.1 | 0.11 | 0 | 100.0 | 0.19 | 0.10 |
| S_4 | 20 | 0.23 | 41 | 67.0 | 0.29 | 7 | 64.1 | 0.49 | 0.34 |
| S_4 | 30 | 0.16 | 17 | 92.7 | 0.19 | 0 | 100.0 | 0.35 | 0.19 |
| S_4 | 40 | 0.12 | 9 | 93.5 | 0.15 | 0 | 100.0 | 0.24 | 0.14 |
| S_4 | 50 | 0.10 | 6 | 93.2 | 0.12 | 0 | 100.0 | 0.20 | 0.11 |
| S_4 | 60 | 0.09 | 1 | 97.1 | 0.11 | 0 | 100.0 | 0.17 | 0.09 |
| S_5 | 20 | 0.24 | 43 | 62.7 | 0.29 | 5 | 76.9 | 0.52 | 0.37 |
| S_5 | 30 | 0.16 | 17 | 92.3 | 0.19 | 0 | 100.0 | 0.32 | 0.18 |
| S_5 | 40 | 0.12 | 18 | 82.7 | 0.15 | 1 | 81.3 | 0.25 | 0.16 |
| S_5 | 50 | 0.10 | 7 | 89.5 | 0.12 | 0 | 100.0 | 0.21 | 0.12 |
| S_5 | 60 | 0.09 | 2 | 96.1 | 0.11 | 0 | 100.0 | 0.17 | 0.09 |
| S_6 | 20 | 0.23 | 23 | 94.3 | 0.29 | 5 | 73.5 | 0.49 | 0.33 |
| S_6 | 30 | 0.16 | 11 | 97.1 | 0.19 | 1 | 90.1 | 0.32 | 0.20 |
| S_6 | 40 | 0.12 | 6 | 96.5 | 0.15 | 0 | 100.0 | 0.26 | 0.14 |
| S_6 | 50 | 0.10 | 3 | 96.3 | 0.12 | 0 | 100.0 | 0.21 | 0.11 |
| S_6 | 60 | 0.09 | 0 | 100.0 | 0.11 | 0 | 100.0 | 0.19 | 0.09 |
| S_7 | 20 | 0.24 | 36 | 76.2 | 0.29 | 5 | 75.0 | 0.50 | 0.34 |
| S_7 | 30 | 0.16 | 13 | 94.2 | 0.19 | 2 | 80.1 | 0.33 | 0.20 |
| S_7 | 40 | 0.12 | 19 | 79.1 | 0.15 | 0 | 100.0 | 0.25 | 0.15 |
| S_7 | 50 | 0.10 | 18 | 74.0 | 0.12 | 0 | 100.0 | 0.22 | 0.11 |
| S_7 | 60 | 0.09 | 6 | 87.7 | 0.11 | 0 | 100.0 | 0.18 | 0.10 |
| F_1 | 20 | 0.24 | 35 | 80.1 | 0.29 | 3 | 88.4 | 0.59 | 0.32 |
| F_1 | 30 | 0.16 | 29 | 76.4 | 0.20 | 3 | 75.6 | 0.32 | 0.22 |
| F_1 | 40 | 0.12 | 24 | 76.2 | 0.15 | 3 | 62.8 | 0.25 | 0.16 |
| F_1 | 50 | 0.10 | 57 | 33.3 | 0.13 | 4 | 48.9 | 0.20 | 0.14 |
| F_1 | 60 | 0.09 | 56 | 33.6 | 0.11 | 2 | 55.0 | 0.17 | 0.11 |
| F_2 | 20 | 0.24 | 32 | 84.6 | 0.29 | 6 | 68.8 | 0.51 | 0.35 |
| F_2 | 30 | 0.16 | 22 | 86.6 | 0.20 | 2 | 82.9 | 0.32 | 0.20 |
| F_2 | 40 | 0.13 | 23 | 74.9 | 0.15 | 1 | 78.4 | 0.27 | 0.15 |
| F_2 | 50 | 0.10 | 45 | 45.4 | 0.13 | 3 | 56.0 | 0.22 | 0.14 |
| F_2 | 60 | 0.09 | 28 | 55.5 | 0.11 | 0 | 100.0 | 0.19 | 0.11 |
| F_3 | 20 | 0.24 | 34 | 80.5 | 0.29 | 10 | 46.2 | 0.54 | 0.34 |
| F_3 | 30 | 0.16 | 21 | 86.0 | 0.20 | 1 | 89.8 | 0.33 | 0.21 |
| F_3 | 40 | 0.13 | 10 | 93.1 | 0.15 | 0 | 100.0 | 0.25 | 0.14 |
| F_3 | 50 | 0.10 | 6 | 91.8 | 0.13 | 0 | 100.0 | 0.22 | 0.12 |
| F_3 | 60 | 0.09 | 9 | 80.3 | 0.11 | 0 | 100.0 | 0.18 | 0.10 |
| F_4 | 20 | 0.24 | 45 | 57.0 | 0.29 | 11 | 37.6 | 0.50 | 0.34 |
| F_4 | 30 | 0.16 | 24 | 82.5 | 0.20 | 0 | 100.0 | 0.32 | 0.19 |
| F_4 | 40 | 0.12 | 16 | 83.0 | 0.15 | 0 | 100.0 | 0.24 | 0.14 |
| F_4 | 50 | 0.10 | 19 | 73.2 | 0.13 | 0 | 100.0 | 0.20 | 0.11 |
| F_4 | 60 | 0.09 | 16 | 69.4 | 0.11 | 0 | 100.0 | 0.18 | 0.10 |
| F_5 | 20 | 0.24 | 55 | 36.1 | 0.29 | 12 | 33.3 | 0.52 | 0.34 |
| F_5 | 30 | 0.16 | 19 | 90.0 | 0.20 | 1 | 91.7 | 0.32 | 0.20 |
| F_5 | 40 | 0.12 | 5 | 97.9 | 0.15 | 0 | 100.0 | 0.26 | 0.13 |
| F_5 | 50 | 0.10 | 12 | 82.8 | 0.13 | 0 | 100.0 | 0.20 | 0.11 |
| F_5 | 60 | 0.09 | 9 | 80.5 | 0.11 | 0 | 100.0 | 0.19 | 0.10 |
| F_6 | 20 | 0.24 | 46 | 54.8 | 0.29 | 11 | 39.8 | 0.56 | 0.36 |
| F_6 | 30 | 0.16 | 32 | 71.3 | 0.20 | 1 | 89.3 | 0.34 | 0.20 |
| F_6 | 40 | 0.12 | 22 | 78.1 | 0.15 | 1 | 83.3 | 0.24 | 0.15 |
| F_6 | 50 | 0.10 | 21 | 67.9 | 0.13 | 1 | 70.2 | 0.22 | 0.13 |
| F_6 | 60 | 0.09 | 4 | 89.8 | 0.11 | 0 | 100.0 | 0.20 | 0.10 |
| F_7 | 20 | 0.24 | 37 | 75.2 | 0.29 | 8 | 55.4 | 0.51 | 0.33 |
| F_7 | 30 | 0.16 | 16 | 94.2 | 0.20 | 0 | 100.0 | 0.34 | 0.19 |
| F_7 | 40 | 0.13 | 10 | 92.5 | 0.15 | 0 | 100.0 | 0.27 | 0.14 |
| F_7 | 50 | 0.10 | 21 | 68.9 | 0.13 | 0 | 100.0 | 0.21 | 0.12 |
| F_7 | 60 | 0.09 | 21 | 61.7 | 0.11 | 0 | 100.0 | 0.18 | 0.10 |

* r are the radii of the patches.† D_5^s , D_1^s , and D_0^s delimit the highest 5%, 1%, and the maximum of all D^s values from all patches in all shuffled data.‡ N_i^m is the number of patches in the measured data for which $D^m > D_i^s$, where $i=5$ or 1.# P_i^N is the probability of finding at least N_i^m number of patches with $D^s > D_i^s$ in the randomly shuffled data, where $i=5$ or 1. The cases with $P_i^N \leq 5\%$ are emphasized in boldface.§ D_0^m is the maximum value of the statistic in the measured data.**Table 11.** Results using the Kuiper statistic V for the *Swift*/BAT sample.

| Obs. | r | V_5^s | N_5^m | P_5^N (%) | V_1^s | N_1^m | P_1^N (%) | V_0^s | V_0^m |
|----------|-----|---------|---------|----------------|---------|---------|----------------|---------|---------|
| T_{90} | 20 | 0.30 | 45 | 59.3 | 0.35 | 9 | 50.9 | 0.54 | 0.37 |
| T_{90} | 30 | 0.20 | 35 | 69.8 | 0.23 | 2 | 84.7 | 0.35 | 0.24 |
| T_{90} | 40 | 0.16 | 42 | 51.8 | 0.18 | 2 | 72.5 | 0.27 | 0.20 |
| T_{90} | 50 | 0.13 | 81 | 18.8 | 0.15 | 17 | 20.6 | 0.22 | 0.17 |
| T_{90} | 60 | 0.12 | 68 | 25.4 | 0.13 | 16 | 19.6 | 0.19 | 0.14 |
| S_1 | 20 | 0.30 | 33 | 83.4 | 0.35 | 5 | 76.6 | 0.61 | 0.41 |
| S_1 | 30 | 0.20 | 32 | 73.1 | 0.24 | 2 | 85.2 | 0.36 | 0.24 |
| S_1 | 40 | 0.16 | 25 | 74.3 | 0.18 | 5 | 56.5 | 0.28 | 0.19 |
| S_1 | 50 | 0.13 | 14 | 80.2 | 0.15 | 1 | 71.0 | 0.23 | 0.16 |
| S_1 | 60 | 0.12 | 10 | 80.2 | 0.13 | 0 | 100.0 | 0.20 | 0.12 |
| S_2 | 20 | 0.30 | 29 | 97.9 | 0.35 | 5 | 78.9 | 0.60 | 0.44 |
| S_2 | 30 | 0.20 | 19 | 91.9 | 0.23 | 0 | 100.0 | 0.36 | 0.23 |
| S_2 | 40 | 0.16 | 19 | 83.3 | 0.18 | 1 | 85.6 | 0.27 | 0.19 |
| S_2 | 50 | 0.13 | 4 | 95.3 | 0.15 | 0 | 100.0 | 0.24 | 0.15 |
| S_2 | 60 | 0.12 | 16 | 72.4 | 0.13 | 1 | 67.3 | 0.21 | 0.14 |
| S_3 | 20 | 0.30 | 37 | 77.8 | 0.35 | 6 | 71.6 | 0.57 | 0.47 |
| S_3 | 30 | 0.20 | 29 | 80.4 | 0.23 | 3 | 79.4 | 0.36 | 0.27 |
| S_3 | 40 | 0.16 | 21 | 79.9 | 0.18 | 0 | 100.0 | 0.27 | 0.17 |
| S_3 | 50 | 0.13 | 9 | 90.6 | 0.15 | 0 | 100.0 | 0.24 | 0.15 |
| S_3 | 60 | 0.12 | 9 | 83.4 | 0.13 | 0 | 100.0 | 0.22 | 0.13 |
| S_4 | 20 | 0.30 | 49 | 49.2 | 0.35 | 9 | 49.7 | 0.58 | 0.43 |
| S_4 | 30 | 0.20 | 43 | 55.3 | 0.24 | 7 | 54.1 | 0.37 | 0.25 |
| S_4 | 40 | 0.16 | 34 | 63.2 | 0.18 | 0 | 100.0 | 0.27 | 0.18 |
| S_4 | 50 | 0.13 | 23 | 70.6 | 0.15 | 2 | 66.0 | 0.23 | 0.16 |
| S_4 | 60 | 0.12 | 10 | 80.9 | 0.13 | 1 | 66.9 | 0.20 | 0.14 |
| S_5 | 20 | 0.30 | 60 | 27.2 | 0.35 | 11 | 39.2 | 0.56 | 0.43 |
| S_5 | 30 | 0.20 | 51 | 44.5 | 0.23 | 2 | 84.1 | 0.35 | 0.24 |
| S_5 | 40 | 0.16 | 57 | 35.7 | 0.18 | 6 | 50.6 | 0.28 | 0.21 |
| S_5 | 50 | 0.13 | 30 | 62.3 | 0.15 | 3 | 57.2 | 0.25 | 0.16 |
| S_5 | 60 | 0.12 | 15 | 75.1 | 0.13 | 1 | 66.8 | 0.19 | 0.14 |
| S_6 | 20 | 0.30 | 31 | 87.5 | 0.35 | 5 | 78.2 | 0.55 | 0.46 |
| S_6 | 30 | 0.20 | 28 | 79.3 | 0.24 | 1 | 91.2 | 0.34 | 0.25 |
| S_6 | 40 | 0.16 | 17 | 86.1 | | | | | |

Table 12. Results using the Anderson–Darling statistic AD for the *Swift*/BAT sample.

| Obs. | r | AD_5^s | N_5^m | P_5^N (%) | AD_1^s | N_1^m | P_1^N (%) | AD_0^s | AD_0^m |
|----------|-----|----------|---------|----------------|----------|---------|----------------|----------|----------|
| | (°) | | | | | | | | |
| T_{90} | 20 | 2.50 | 61 | 26.6 | 3.90 | 8 | 52.0 | 12.96 | 4.80 |
| T_{90} | 30 | 2.50 | 87 | 11.8 | 3.92 | 17 | 19.2 | 13.16 | 4.87 |
| T_{90} | 40 | 2.49 | 115 | 6.5 | 3.86 | 25 | 13.3 | 12.67 | 5.55 |
| T_{90} | 50 | 2.50 | 145 | 5.4 | 3.87 | 56 | 3.5 | 10.71 | 7.04 |
| T_{90} | 60 | 2.46 | 169 | 4.9 | 3.84 | 44 | 6.3 | 10.53 | 6.97 |
| S_1 | 20 | 2.50 | 29 | 86.7 | 3.89 | 6 | 65.9 | 12.08 | 6.41 |
| S_1 | 30 | 2.51 | 7 | 97.8 | 3.89 | 0 | 100.0 | 11.96 | 3.29 |
| S_1 | 40 | 2.50 | 10 | 88.4 | 3.92 | 0 | 100.0 | 12.39 | 3.85 |
| S_1 | 50 | 2.48 | 2 | 96.9 | 3.85 | 0 | 100.0 | 10.35 | 2.92 |
| S_1 | 60 | 2.51 | 0 | 100.0 | 3.92 | 0 | 100.0 | 10.57 | 1.91 |
| S_2 | 20 | 2.50 | 30 | 83.1 | 3.90 | 7 | 60.3 | 11.14 | 6.48 |
| S_2 | 30 | 2.48 | 8 | 98.4 | 3.84 | 0 | 100.0 | 12.69 | 3.01 |
| S_2 | 40 | 2.53 | 7 | 92.1 | 3.93 | 0 | 100.0 | 13.14 | 3.55 |
| S_2 | 50 | 2.47 | 1 | 96.4 | 3.86 | 0 | 100.0 | 18.71 | 2.89 |
| S_2 | 60 | 2.51 | 0 | 100.0 | 3.94 | 0 | 100.0 | 11.85 | 1.88 |
| S_3 | 20 | 2.47 | 33 | 79.1 | 3.83 | 10 | 43.0 | 13.25 | 6.28 |
| S_3 | 30 | 2.48 | 11 | 96.4 | 3.85 | 0 | 100.0 | 11.75 | 3.45 |
| S_3 | 40 | 2.46 | 7 | 94.1 | 3.85 | 0 | 100.0 | 13.16 | 3.21 |
| S_3 | 50 | 2.48 | 1 | 98.5 | 3.83 | 0 | 100.0 | 12.57 | 3.05 |
| S_3 | 60 | 2.45 | 0 | 100.0 | 3.80 | 0 | 100.0 | 11.23 | 2.14 |
| S_4 | 20 | 2.49 | 42 | 63.8 | 3.88 | 8 | 53.3 | 11.58 | 6.46 |
| S_4 | 30 | 2.49 | 19 | 87.5 | 3.89 | 0 | 100.0 | 11.74 | 3.88 |
| S_4 | 40 | 2.48 | 10 | 91.1 | 3.89 | 0 | 100.0 | 12.31 | 3.28 |
| S_4 | 50 | 2.50 | 2 | 97.2 | 3.85 | 0 | 100.0 | 12.07 | 3.52 |
| S_4 | 60 | 2.48 | 1 | 95.1 | 3.82 | 0 | 100.0 | 12.78 | 2.48 |
| S_5 | 20 | 2.49 | 51 | 43.3 | 3.87 | 7 | 58.3 | 12.74 | 7.20 |
| S_5 | 30 | 2.46 | 23 | 82.3 | 3.83 | 3 | 69.4 | 11.97 | 4.52 |
| S_5 | 40 | 2.49 | 13 | 86.0 | 3.87 | 0 | 100.0 | 13.04 | 3.15 |
| S_5 | 50 | 2.49 | 5 | 88.5 | 3.88 | 0 | 100.0 | 15.15 | 3.59 |
| S_5 | 60 | 2.49 | 1 | 96.2 | 3.88 | 0 | 100.0 | 10.74 | 2.62 |
| S_6 | 20 | 2.49 | 28 | 87.5 | 3.88 | 8 | 54.1 | 13.33 | 6.60 |
| S_6 | 30 | 2.49 | 9 | 96.4 | 3.89 | 0 | 100.0 | 14.20 | 3.21 |
| S_6 | 40 | 2.48 | 8 | 93.3 | 3.85 | 0 | 100.0 | 12.80 | 3.38 |
| S_6 | 50 | 2.49 | 1 | 97.8 | 3.88 | 0 | 100.0 | 11.80 | 3.08 |
| S_6 | 60 | 2.54 | 0 | 100.0 | 3.94 | 0 | 100.0 | 12.91 | 2.12 |
| S_7 | 20 | 2.52 | 39 | 67.6 | 3.93 | 8 | 52.0 | 11.15 | 6.65 |
| S_7 | 30 | 2.53 | 16 | 89.4 | 3.96 | 2 | 75.8 | 12.60 | 4.10 |
| S_7 | 40 | 2.53 | 11 | 86.7 | 3.98 | 0 | 100.0 | 14.02 | 3.30 |
| S_7 | 50 | 2.47 | 1 | 98.3 | 3.86 | 0 | 100.0 | 14.95 | 3.37 |
| S_7 | 60 | 2.49 | 0 | 100.0 | 3.86 | 0 | 100.0 | 11.64 | 2.25 |
| F_1 | 20 | 2.48 | 56 | 35.6 | 3.86 | 12 | 34.4 | 10.97 | 7.79 |
| F_1 | 30 | 2.50 | 62 | 30.3 | 3.86 | 8 | 44.3 | 11.71 | 4.77 |
| F_1 | 40 | 2.50 | 83 | 18.6 | 3.89 | 4 | 52.6 | 11.19 | 4.42 |
| F_1 | 50 | 2.51 | 94 | 16.3 | 3.89 | 23 | 14.0 | 10.58 | 5.71 |
| F_1 | 60 | 2.49 | 101 | 15.3 | 3.87 | 22 | 14.8 | 10.94 | 6.01 |
| F_2 | 20 | 2.46 | 48 | 50.6 | 3.84 | 12 | 32.5 | 12.40 | 8.07 |
| F_2 | 30 | 2.48 | 49 | 45.9 | 3.83 | 9 | 42.3 | 11.99 | 5.42 |
| F_2 | 40 | 2.52 | 66 | 27.5 | 3.96 | 4 | 50.6 | 13.41 | 4.72 |
| F_2 | 50 | 2.51 | 78 | 21.8 | 3.90 | 22 | 14.9 | 11.93 | 5.33 |
| F_2 | 60 | 2.54 | 76 | 21.3 | 3.96 | 12 | 22.0 | 13.67 | 5.36 |
| F_3 | 20 | 2.50 | 45 | 56.5 | 3.87 | 9 | 47.1 | 11.45 | 7.17 |
| F_3 | 30 | 2.48 | 28 | 73.2 | 3.86 | 5 | 57.0 | 12.74 | 4.63 |
| F_3 | 40 | 2.52 | 31 | 60.3 | 3.93 | 0 | 100.0 | 13.19 | 3.67 |
| F_3 | 50 | 2.51 | 49 | 38.4 | 3.89 | 6 | 37.4 | 13.18 | 4.69 |
| F_3 | 60 | 2.50 | 36 | 46.8 | 3.83 | 1 | 58.6 | 14.16 | 4.27 |
| F_4 | 20 | 2.52 | 50 | 45.2 | 3.91 | 6 | 65.5 | 11.75 | 6.67 |
| F_4 | 30 | 2.51 | 27 | 76.5 | 3.91 | 5 | 57.5 | 12.44 | 4.74 |
| F_4 | 40 | 2.47 | 34 | 58.2 | 3.84 | 0 | 100.0 | 11.81 | 3.45 |
| F_4 | 50 | 2.48 | 47 | 39.6 | 3.86 | 2 | 55.0 | 13.23 | 4.13 |
| F_4 | 60 | 2.52 | 28 | 50.9 | 3.97 | 0 | 100.0 | 12.40 | 3.94 |
| F_5 | 20 | 2.49 | 62 | 26.2 | 3.87 | 7 | 57.8 | 12.82 | 6.02 |
| F_5 | 30 | 2.50 | 31 | 70.3 | 3.88 | 5 | 58.1 | 11.25 | 4.50 |
| F_5 | 40 | 2.48 | 17 | 81.2 | 3.85 | 0 | 100.0 | 13.92 | 3.03 |
| F_5 | 50 | 2.48 | 39 | 48.7 | 3.86 | 1 | 64.8 | 12.88 | 3.96 |
| F_5 | 60 | 2.50 | 24 | 57.3 | 3.94 | 0 | 100.0 | 11.20 | 3.90 |
| F_6 | 20 | 2.48 | 50 | 44.7 | 3.87 | 13 | 29.5 | 11.23 | 7.74 |
| F_6 | 30 | 2.49 | 38 | 61.3 | 3.87 | 6 | 52.9 | 12.39 | 5.58 |
| F_6 | 40 | 2.50 | 51 | 42.1 | 3.85 | 3 | 59.3 | 12.22 | 4.20 |
| F_6 | 50 | 2.52 | 63 | 30.0 | 3.89 | 14 | 23.9 | 12.14 | 4.94 |
| F_6 | 60 | 2.48 | 58 | 31.9 | 3.89 | 3 | 41.4 | 12.19 | 4.93 |
| F_7 | 20 | 2.49 | 45 | 55.8 | 3.85 | 8 | 53.3 | 12.67 | 6.64 |
| F_7 | 30 | 2.51 | 28 | 74.1 | 3.94 | 6 | 50.5 | 12.23 | 5.15 |
| F_7 | 40 | 2.51 | 30 | 63.7 | 3.91 | 0 | 100.0 | 13.18 | 3.46 |
| F_7 | 50 | 2.51 | 48 | 40.3 | 3.91 | 2 | 54.6 | 13.64 | 4.01 |
| F_7 | 60 | 2.48 | 30 | 49.4 | 3.87 | 1 | 54.4 | 11.32 | 4.11 |

* r are the radii of the patches.† AD_5^s , AD_1^s and AD_0^s delimit the highest 5%, 1%, and the maximum of all AD^s values from all patches in all shuffled data.‡ N_i^m is the number of patches in the measured data for which $AD^m > AD_i^s$, where $i=5$ or 1.# P_i^N is the probability of finding at least N_i^m number of patches with $AD^s > AD_i^s$ in the randomly shuffled data, where $i=5$ or 1. The cases with $P_i^N \leq 5\%$ are emphasized in boldface.§ AD_0^m is the maximum value of the statistic in the measured data.**Table 13.** Results using the χ^2 statistic for the *Swift*/BAT sample.

| Obs. | r | χ_5^{2s} | N_5^m | P_5^N (%) | χ_1^{2s} | N_1^m | P_1^N (%) | χ_0^{2s} | χ_0^{2m} |
|----------|-----|---------------|---------|----------------|---------------|---------|----------------|---------------|---------------|
| | (°) | | | | | | | | |
| T_{90} | 20 | 21.09 | 77 | 3.1 | 42.93 | 6 | 59.4 | 113.50 | 50.62 |
| T_{90} | 30 | 20.97 | 62 | 30.0 | 28.02 | 25 | 10.7 | 67.82 | 41.37 |
| T_{90} | 40 | 17.90 | 136 | 1.7 | 23.25 | 52 | 1.8 | 55.28 | 54.61 |
| T_{90} | 50 | 17.07 | 155 | 2.0 | 21.98 | 48 | 3.3 | 47.86 | 40.90 |
| T_{90} | 60 | 16.66 | 181 | 2.3 | 21.27 | 61 | 2.3 | 44.66 | 32.07 |
| S_1 | 20 | 25.41 | 44 | 67.4 | 43.98 | 0 | 100.0 | 155.46 | 43.27 |
| S_1 | 30 | 21.11 | 62 | 30.2 | 29.35 | 8 | 40.9 | 73.25 | 47.15 |
| S_1 | 40 | 18.53 | 97 | 11.2 | 24.70 | 35 | 7.7 | 56.10 | 46.78 |
| S_1 | 50 | 17.25 | 118 | 8.7 | 22.54 | 52 | 3.6 | 45.28 | 33.77 |
| S_1 | 60 | 16.63 | 142 | 4.8 | 21.10 | 65 | 1.9 | 41.06 | 33.19 |
| S_2 | 20 | 32.63 | 38 | 80.4 | 49.05 | 8 | 49.5 | 143.29 | 59.63 |
| S_2 | 30 | 22.68 | 45 | 53.1 | 31.71 | 6 | 44.7 | 71.67 | 41.02 |
| S_2 | 40 | 19.27 | 48 | 47.4 | 25.48 | 4 | 52.9 | 69.28 | 27.70 |
| S_2 | 50 | 17.58 | 54 | 50.8 | 22.91 | 1 | 66.7 | 53.34 | 24.79 |
| S_2 | 60 | 16.29 | 20 | 68.9 | 20.67 | 2 | 57.2 | 38.91 | 22.63 |
| S_3 | 20 | 31.70 | 59 | 26.8 | 48.46 | 13 | 33.8 | 142.35 | 61.14 |
| S_3 | 30 | 21.90 | 46 | 54.2 | 31.10 | 14 | 28.1 | 71.31 | 39.32 |
| S_3 | 40 | 17.98 | 101 | 9.2 | 24.49 | 22 | 15.7 | 66.47 | 33.88 |
| S_3 | 50 | 16.19 | 96 | 14.1 | 21.35 | 8 | 34.6 | 45.15 | 22.69 |
| S_3 | 60 | 15.00 | 59 | 32.2 | 19.24 | 0 | 100.0 | 39.60 | 19.18 |
| S_4 | 20 | 36.07 | 42 | 68.7 | 53.34 | 9 | 45.0 | 158.43 | 69.23 |
| S_4 | 30 | 24.31 | 54 | 40.0 | 35.12 | 2 | 63.5 | 97.67 | 35.70 |
| S_4 | 40 | 19.98 | 51 | 43.8 | 26.52 | 10 | 33.3 | 52.70 | 33.02 |
| S_4 | 50 | 17.67 | 76 | 22.5 | 22.74 | 4 | 49.0 | 50.20 | 23.53 |
| S_4 | 60 | 16.21 | 35 | 50.8 | 20.48 | 0 | 100.0 | 44.64 | 19.98 |
| S_5 | 20 | 36.50 | 40 | 71.8 | 53.03 | 8 | 50.8 | 157.77 | 69.19 |
| S_5 | 30 | 24.24 | 56 | 39.0 | 34.98 | 0 | 100.0 | 87.36 | 34.89 |
| S_5 | 40 | 20.00 | 45 | 50.4 | 26.68 | 5 | | | |

REFERENCES

- Abbott B. P., et al., 2017a, Phys. Rev. Lett., 119, 161101
 Abbott B. P., et al., 2017b, ApJ, 848, L13
 Abbott B. P., et al., 2017c, ApJ, 848, L12
 Akrami Y., Fantaye Y., Shafieloo A., Eriksen H. K., Hansen F. K., Banday A. J., Górski K. M., 2014, ApJ, 784, L42
 Anderson, T. W., & Darling, D. A., 1952, The Annals of Mathematical Statistics, 23, 193
 Appleby S., Shafieloo A., Johnson A., 2015, ApJ, 801, 76
 Appleby S., Shafieloo A., 2014, J. Cosmology Astropart. Phys., 10, 070
 Atwood W. B., GLAST Collaboration, 1994, Nuclear Instruments and Methods in Phys., 342, 302
 Avila F., Novaes C. P., Bernui A., de Carvalho E., 2018, arXiv:1806.04541
 Bagoly Z., Mészáros A., Horváth I., Balázs L. G., Mészáros P., 1998, ApJ, 498, 342
 Bagoly Z., Borgonovo L., Mészáros A., Balázs L. G., Horváth I., 2009, A&A, 493, 51
 Balázs L. G., Mészáros A., Horváth I., Vavrek R., 1999, A&AS, 138, 417
 Balázs L. G., Bagoly Z., Hakkila J. E., Horváth I., Kóbori J., Rácz I. I., Tóth L. V., 2015, MNRAS, 452, 2236
 Balázs L. G., Bagoly Z., Horváth I., Mészáros A., Mészáros P., 2003, A&A, 401, 129
 Balázs L. G., Rejtő L., Tusnády G., 2018, MNRAS, 473, 3169
 Balázs L. G., Mészáros A., Horváth I., 1998, A&A, 339, 1
 Barthelmy S. D., et al., 2005, Space Sci. Rev., 120, 143
 Berger E., 2014, ARA&A, 52, 43
 Bernui A., Ferreira I. S., Wuensche C. A., 2008, ApJ, 673, 968
 Borgonovo L., Björnsson C.-I., 2006, ApJ, 652, 1423
 Briggs M. S., et al., 1996, ApJ, 459, 40
 Cline D. B., Czerny B., Matthey C., Janiuk A., Otwinowski S., 2005, ApJ, 633, L73
 Clowes R. G., Harris K. A., Raghunathan S., Campusano L. E., Söchting I. K., Graham M. J., 2013, MNRAS, 429, 2910
 Colgate S. A., 1968, CaJPh, 46, S476
 Colin J., Mohayaee R., Sarkar S., Shafieloo A., 2011, MNRAS, 414, 264
 Dai Z., Daigne F., Mészáros P., 2017, Space Sci. Rev., 212, 409
 Darling, D. A., 1957, The Annals of Mathematical Statistics, 28, 823
 Eichler D., Livio M., Piran T., Schramm D. N., 1989, Nature, 340, 126
 Feindt U., et al., 2013, A&A, 560, A90
 Fernández-Cobos R., Vielva P., Pietrobon D., Balbi A., Martínez-González E., Barreiro R. B., 2014, MNRAS, 441, 2392
 Fishman G. J., Meegan C. A., Parnell T. A., Wilson R. B., Paciesas W., Mateson J. L., Cline T. L., Teegarden B. J., 1985, 19th Intern. Cosmic Ray Conf., 3, 343
 Fishman G. J., et al., 1994, ApJS, 92, 229
 Frith W. J., Shanks T., Outram P. J., 2005a, MNRAS, 361, 701
 Frith W. J., Outram P. J., Shanks T., 2005b, MNRAS, 364, 593
 Fruchter A. S., et al., 2006, Nature, 441, 463
 Gan L.-x., Zou Y.-c., Dai Z.-g., 2016, Chinese Astron. Astrophys., 40, 12
 Gehrels N., Chipman E., Kniffen D. A., 1993, A&AS, 97, 5
 Gehrels N., et al., 2004, ApJ, 611, 1005
 Goldstein A., et al., 2012, ApJS, 199, 19
 Gomboc A., 2012, Contemporary Phys., 53, 339
 Gott J. R., III, Jurić M., Schlegel D., Hoyle F., Vogeley M., Tegmark M., Bahcall N., Brinkmann J., 2005, ApJ, 624, 463
 Gruber D., et al., 2014, ApJS, 211, 12
 Hinshaw G., Branday A. J., Bennett C. L., Gorski K. M., Kogut A., Lineweaver C. H., Smoot G. F., Wright E. L., 1996, ApJ, 464, L25
 Hogg D. W., Eisenstein D. J., Blanton M. R., Bahcall N. A., Brinkmann J., Gunn J. E., Schneider D. P., 2005, ApJ, 624, 54
 Horváth I., Hakkila J., Bagoly Z., 2014, A&A, 561, L12
 Horváth I., Bagoly Z., Hakkila J., Tóth L. V., 2015, A&A, 584, A48
 Javanmardi B., Porciani C., Kroupa P., Pflamm-Altenburg J., 2015, ApJ, 810, 47
 Javanmardi B., Kroupa P., 2017, A&A, 597, A120
 Kashlinsky A., Atrio-Barandela F., Kocevski D., Ebeling H., 2008, ApJ, 686, L49
 Kolmogorov, A., 1933, Giornale dell'Istituto Italiano degli Attuari, 4, 83
 Kouveliotou C., Meegan C. A., Fishman G. J., Bhat N. P., Briggs M. S., Koshut T. M., Paciesas W. S., Pendleton G. N., 1993, ApJ, 413, L101
 Kouveliotou C., Wijers R. A. M. J., Woosley S., 2012, Gamma-ray Bursts, Cambridge, UK: Cambridge University Press
 Kroupa P., 2015, Canadian Journal of Physics, 93, 169
 Kuiper, N. H., 1960, Proc. Koninkl. Nederl. Akad. Van Wetenschappen, Series A, 63, 38
 Kumar P., Zhang B., 2015, Phys. Rep., 561, 1
 Landsman, W. B., 1993, Astronomical Data Analysis Software and Systems II, A.S.P. Conference Series, ed. R. J. Hanisch, R. J. V. Brissenden, and Jeannette Barnes, 52, 246
 Li M.-H., Lin H.-N., 2015, A&A, 582, A111
 Litvin V. F., Matveev S. A., Mamedov S. V., Orlov V. V., 2001, Astron. Lett., 27, 416
 Mészáros A., 2017, Proc. of the IAU, 324, 89
 Mészáros A., 2018, Proc. of the IAU, 333, 203
 Mészáros A., Bagoly Z., Horváth I., Balázs L. G., Vavrek R., 2000a, ApJ, 539, 98
 Mészáros A., Bagoly Z., Vavrek R., 2000b, A&A, 354, 1
 Mészáros A., Balázs L. G., Bagoly Z., Veres P., 2009a, Baltic Astron., 18, 293
 Mészáros A., Balázs L. G., Bagoly Z., Veres P., 2009b, AIP Conf. Proc., 1133, 483
 Mészáros A., Štoček J., 2003, A&A, 403, 443
 Mészáros P., 2006, Rep. on Prog. in Phys., 69, 2259
 Magliocchetti M., Ghirlanda G., Celotti A., 2003, MNRAS, 343, 255
 Meegan C. A., Fishman G. J., Wilson R. B., Paciesas W. S., Pendleton G. N., Horack J. M., Brock M. N., Kouveliotou C., 1992, Nature, 355, 143
 Meegan C. A., et al., 1996, ApJS, 106, 65
 Meegan C. A., et al., 1998, AIP Conf. Proc., 428, 3
 Meegan C., et al., 2009, ApJ, 702, 791
 Nadathur S., 2013, MNRAS, 434, 398
 Narayana Bhat P., et al., 2016, ApJS, 223, 28
 Paciesas W. S., et al., 1999, ApJS, 122, 465
 Paciesas W. S., et al., 2012, ApJS, 199, 18
 Paczynski B., 1986, ApJ, 308, L43
 Pettitt, A. N., 1976, Biometrika, 63, 161
 Piran T., 2004, Rev. of Modern Phys., 76, 1143
 Planck Collaboration, et al., 2014, A&A, 571, A23
 Planck Collaboration, et al., 2016, A&A, 594, A16
 Press, W. H., Teukolsky, S. A., Vetterling, W. T., & Flannery, B. P., 2007, Numerical Recipes: The Art of Scientific Computing, Third Edition, Cambridge, UK: Cambridge University Press
 R Core Team, 2013, R: A Language and Environment for Statistical Computing, Vienna, Austria: R Foundation for Statistical Computing
 Raikov A. A., Orlov V. V., Bektev O. B., 2010, Astrophysics, 53, 396
 Řípa J., Shafieloo A., 2017, ApJ, 851, 15
 Rudnick L., Brown S., Williams L. R., 2007, ApJ, 671, 40
 Scholz F., 2012, adk: Anderson-Darling K-Sample Test and Combinations of Such Tests, R package version 1.0-2, CRAN

- Scrimgeour M. I., et al., 2012, MNRAS, 425, 116
- Shafieloo A., 2012a, J. Cosmology Astropart. Phys., 5, 024
- Shafieloo A., 2012b, J. Cosmology Astropart. Phys., 8, 002
- Shafieloo A., Clifton T., Ferreira P., 2011, J. Cosmology Astropart. Phys., 8, 017
- Shirokov S. I., Raikov A. A., Baryshev Y. V., 2017, Astrophysics, 60, 484
- Smirnov, N. V., 1939, Bulletin Mathématique de l'Université de Moscou, 2, 3
- Sokolov I. V., Castro-Tirado A. J., Zhelenkova O. P., Solovyev I. A., Verkhodanov O. V., Sokolov V. V., 2018, Astrophysical Bulletin, 73, 111
- Tarnopolski M., 2017, MNRAS, 472, 4819
- Tegmark M., Hartmann D. H., Briggs M. S., Meegan C. A., 1996, ApJ, 468, 214
- Tiwari P., Jain P., 2018, arXiv:1809.01270
- Ukwatta T. N., Woźniak P. R., 2016, MNRAS, 455, 703
- Vavrek R., Balázs L. G., Mészáros A., Horváth I., Bagoly Z., 2008, MNRAS, 391, 1741
- Vedrenne G., Atteia J.-L., 2009, Gamma-Ray Bursts: The Brightest Explosions in the Universe, Springer Praxis Books, Chichester, UK: Praxis Publishing Ltd.
- Veres P., Bagoly Z., Horváth I., Balázs L. G., Mészáros A., Kelen J., 2010, AIP Conf. Proc., 1279, 457
- von Kienlin A., et al., 2014, ApJS, 211, 13
- Willingale R., Mészáros P., 2017, Space Sci. Rev., 207, 63
- Woolsey S. E., Bloom J. S., 2006, ARA&A, 44, 507

This paper has been typeset from a TeX/LaTeX file prepared by the author.